# UNIVERSITY OF CINCINNATI

**Date:** August 12, 2008

I, Anthony John Jasper,

**hereby submit this work as part of the requirements for the degree of:**

Master of Science

**in:**

Environmental Science

**It is entitled:**

Impact of Nanoparticles and Natural Organic Matter on the Removal of Organic Pollutants by Activated Carbon Adsorption

**This work and its defense approved by:**

**Chair:** Dr. George Sorial

Dr. Margaret Kupferle

Dr. Dionysios Dionysiou

Craig Patterson

# IMPACT OF NANOPARTICLES AND NATURAL ORGANIC MATTER ON THE REMOVAL OF ORGANIC POLLUTANTS BY ACTIVATED CARBON ADSORPTION

A thesis submitted in partial fulfillment of
the requirement for the degree of

## MASTER OF SCIENCE

In the Department of Civil & Environmental Engineering,
College of Engineering at the University of Cincinnati

August 2008

Prepared by:

Anthony John Jasper

B.S. University of Dayton, 2006

Thesis Committee Chair:
Dr. George Sorial U.C

Thesis Committee Members:
Dr. Dionysios D. Dionysiou U.C.
Dr. Margaret Kupferle U.C.
Craig L. Patterson, P.E. USEPA

## Abstract

Isotherm experiments evaluating trichloroethylene (TCE) adsorption onto powdered activated carbon (PAC) were conducted in the presence and absence of three commercially available nanomaterials— Iron oxide ($Fe_2O_3$), titanium dioxide ($TiO_2$), and silicon dioxide ($SiO_2$). Isotherm experiments were also conducted in the presence and absence of natural organic matter (NOM), in the form of humic acid, to more closely model natural water conditions. Nanoparticles at two concentration levels (0.5 and 1.0 mg/L for $Fe_2O_3$ and $TiO_2$, and 5.0 and 10 mg/L for $SiO_2$) were considered. Particle size distribution (PSD) of the nanoparticle solutions was analyzed with time in order to determine the nanoparticle size range of each solution. Aggregation of $Fe_2O_3$ and $TiO_2$ was noticed, while none was observed for $SiO_2$ solutions. Adsorption isotherm experiments were conducted at three initial TCE concentrations, two nanoparticle concentrations, and with varying amounts of powdered activated carbon (PAC). Isotherm data showed a higher degree of TCE adsorption in the presence of $Fe_2O_3$ and $TiO_2$ nanoparticles, regardless of concentration. $Fe_2O_3$ and $TiO_2$ nanoparticles alone were observed to act as adsorption sites for TCE by removing up to 60% of TCE from the aqueous phase. Silica appeared to have no impact on TCE adsorption at either concentration used, except in the presence of humic acid. GAC column experiments were also conducted to determine how the presence of silica nanoparticles impacted the breakthrough behavior of TCE in an adsorber bed.



**Keywords** Activated Carbon, Adsorption, Aggregation, Nanoparticles, Particle Size Distribution (PSD), Trichloroethylene (TCE)

## Acknowledgments

*This work was funded by a research grant (Contract No. EP-C-04-034; Work Assignment No. 3-03 and 4-03) from the United States Environmental Protection Agency (Office of Research and Development). This work; however, does not necessarily reflect the views of the EPA and no official endorsement should be inferred.*

I would like to acknowledge the USEPA, as well as Shaw Environmental, Inc. for funding this project and allowing me to use their facilities. More specifically, I would like to thank Craig Patterson (EPA), Rajib Sinha (Shaw), and Radha Krishnan (Shaw) for guidance on this project. I would also like to express my gratitude and appreciation for my advisor and mentor, Dr. George Sorial for lending his support and direction for this work. I would also like to thank my thesis committee; Dr. Dionysios Dionysiou, Dr. Margaret Kupferle, and Craig Patterson. Finally, it is important to express my gratitude for the staff at the T&E Facility, such as Brad Smith, John Brannon, Harmon Morress, Tim Gray, and Jill Webster, who were a tremendous help to myself and this project.

## Table of Contents


Title Page i

Abstract ii

Acknowledgements iv

Table of Contents v

List of Tables vii

List of Figures viii

1.0 Introduction 1

1.1 Problem Statement 1
1.2 Objectives 2

2.0 Literature Review 4

2.1 Environmental Nanotechnology 4
2.2 Organic Pollutant Removal by Activated Carbon Adsorption 6
2.3 Impact of NOM on Micropollutant Adsorption 11
2.4 Trichloroethylene 15
2.5 Nanoparticles as Adsorption Sites 17

3.0 Experimental and Analytical Methodology 20

3.1 Materials 20

3.1.1 Adsorbents 20
3.1.2 Nanomaterials 20
3.1.3 Adsorbates 21
3.1.4 Water 21
3.1.5 Glassware and Analytical Instruments 22

3.2 Methods 23

3.2.1 Particle Size Distribution Analysis 23
3.2.2 Adsorption Isotherm Experiments 24
3.2.3 GAC Column Studies 25

3.3 Sample Analysis 26

3.3.1 TCE Analysis 26
3.3.2 Humic Acid Analysis 27
3.3.3 Particle Size Distribution Analysis 27

3.4 Calculation Procedure of Experimental Samples 28

3.4.1 TCE Concentration 28
3.4.2 Humic Acid Concentration 28
3.4.3 Adsorption Isotherm Calculations 29
3.4.4 GAC Column Calculations 30

4.0 Particle Size Distribution Experimental Results 31

4.1 Particle Size Distribution 31
4.2 Particle Size Distribution for $SiO_2$ 32
4.3 Particle Size Distribution for $TiO_2$ 32
4.4 Particle Size Distribution for $Fe_2O_3$ 39

5.0 Adsorption Isotherm Experimental Results 47

5.1 Single Component Adsorption of TCE 47
5.2 Impact of NOM on TCE Adsorption 52

6.0 GAC Column Experimental Results 59

7.0 Conclusions and Recommendations 67

7.1 Particle Size Distribution 68
7.2 Adsorption Isotherm Experiments 69
7.3 GAC Column Breakthrough Experiments 71
7.4 Recommendations for Future Work 71

8.0 References 73

Appendices 80

Appendix 1: $C_e$ (µg/L TCE) vs. $Q_e$ (µg TCE/mg PAC)
Data for Adsorption Isotherm Experiments 81
Appendix 2: SOP for Conducting Adsorption Isotherm Experiments 85
Appendix 3: SOP for Particle Size Distribution Analysis 87
Appendix 4: Quality Control Procedures for Critical Target Paramters 88

## List of Tables

**Table 5.1** Freundlich adsorption isotherm parameters for TCE adsorption on powdered activated carbon in the absence of Humic Acid_____52

**Table 5.2** Freundlich adsorption isotherm parameters for TCE adsorption on powdered activated carbon in the presence of Humic Acid_____58

## List of Figures

**Figure 3.1** GAC Adsorber setup at EPA T&E Facility 26

**Figure 4.1** Particle size distribution of 0.5 mg/L $TiO_2$ solutions left stationary of bench-top 33

**Figure 4.2** Particle size distribution of 1.0 mg/L $TiO_2$ solutions left stationary of bench-top 34

**Figure 4.3** Particle size distribution for 0.5 mg/L $TiO_2$ solutions placed in a rotary tumbler 34

**Figure 4.4** Particle size distribution for 1.0 mg/L $TiO_2$ solutions placed in a rotary tumbler 35

**Figure 4.5** Particle size distribution for 0.5 mg/L $TiO_2$ solutions permanently maintained in a rotary tumbler 37

**Figure 4.6** Particle size distribution for 0.5 mg/L $TiO_2$ solutions permanently maintained in a rotary tumbler 37

**Figure 4.7** Particle size distribution for 1.0 mg/L $TiO_2$ solutions permanently maintained in a rotary tumbler 38

**Figure 4.8** Particle size distribution for 1.0 mg/L $TiO_2$ solutions permanently maintained in a rotary tumbler 38

**Figure 4.9** Mean particle diameter for 0.5 & 1.0 mg/L $TiO_2$ solutions permanently maintained in a rotary tumbler 39

**Figure 4.10** Particle size distribution of 0.5 mg/L $Fe_2O_3$ solutions left stationary on bench-top 40

**Figure 4.11** Particle size distribution for 1.0 mg/L $Fe_2O_3$ solutions left stationary on bench-top 41

**Figure 4.12** Particle size distribution for 0.5 mg/L $Fe_2O_3$ solutions placed in a rotary tumbler 41

**Figure 4.13** Particle size distribution for 0.5 mg/L $Fe_2O_3$ solutions placed in a rotary tumbler 42

**Figure 4.14** Particle size distribution for 1.0 mg/L $Fe_2O_3$ solutions placed in a rotary tumbler 42

**Figure 4.15** Particle size distribution for 1.0 mg/L $Fe_2O_3$ solutions placed in a rotary tumbler 43

**Figure 4.16** Particle size distribution for 0.5 mg/L $Fe_2O_3$ solutions permanently maintained in a rotary tumbler 44

**Figure 4.17** Particle size distribution for 0.5 mg/L $Fe_2O_3$ solutions permanently maintained in a rotary tumbler 45

**Figure 4.18** Particle size distribution for 1.0 mg/L $Fe_2O_3$ solutions permanently maintained in a rotary tumbler 45

**Figure 4.19** Particle size distribution for 1.0 mg/L $Fe_2O_3$ solutions permanently maintained in a rotary tumbler 46

**Figure 5.1** Adsorption isotherm of TCE in nanopure water 48

**Figure 5.2** Adsorption isotherms of TCE in the presence of $SiO_2$ 49

**Figure 5.3** Adsorption isotherms of TCE in the presence of $TiO_2$ 50

**Figure 5.4** Adsorption isotherms of TCE in the presence of $Fe_2O_3$ 51

**Figure 5.5** Adsorption isotherms of TCE in nanopure water containing 5 mg/L humic acid 53

**Figure 5.6** Adsorption isotherms for TCE in the presence of 5 mg/L humic acid and $SiO_2$ 54

**Figure 5.7** Adsorption isotherms for TCE in the presence of 5 mg/L humic acid and $TiO_2$ 55

**Figure 5.8** Adsorption isotherms for TCE in the presence of 5 mg/L humic acid and $Fe_2O_3$ 56

**Figure 5.9** Adsorption isotherms for humic acid in the presence of TCE and in the presence and absence of nanomaterials 57

**Figure 6.1** Breakthrough plot for TCE in nanopure water and water containing 5 mg/L $SiO_2$ versus ETDOT modeling prediction 63

**Figure 6.2** Influent pH data for the breakthrough experiments shown in Figure 6.1 64

**Figure 6.3** Influent TCE concentration data for the breakthrough experiments shown in Figure 6.1 65

**Figure 6.4** Flowrate data for the breakthrough experiments shown in Figure 6.1 66

## 1.0 Introduction

### 1.1 Problem Statement

Activated carbon is an effective adsorbent and is widely used in the removal of organic contaminants from potable drinking water sources. Drinking water treatment relies heavily on the use granular activated carbon (GAC), which can reduce organic contaminants to undetectable limits and prevent their discharge back into the environment (Stenzel and Gupta, 1995). Trichloroethylene (USEPA MCL: 5 µg/L) is a common organic pollutant that can be effectively removed from drinking water using activated carbon. However, there are many factors that complicate the design and implementation of an activated carbon treatment system. The most influential factor is the presence of natural organic matter (NOM), which can significantly reduce the removal of organic pollutants by causing pore blockage within the activated carbon and competing with the organic contaminants for adsorption sites (Kilduff and Karanfil, 2002). The development of commercially available nanomaterials also has the potential to adversely impact the removal of organic contaminants using activated carbon. Mass production of these nanoparticles, and the subsequent use and disposal of nanomaterials will inevitably lead to their appearance in air, water, and soils (Weisner, 2006). Various nanoparticles have been observed in many studies to act as adsorption sites for a wide range of pollutants. Therefore, nanomaterials present in drinking water sources could potentially adsorb organic micropollutants, which may adversely effect the removal of such compounds in an activated carbon treatment system.

## 1.2 Objectives

The primary objective of this study is to evaluate the impact of the presence of nanomaterials on the effectiveness of GAC adsorption. It is expected that the presence of nanoparticles in water could hinder the GAC application due to the aggregation of nanoparticles, which could act as an adsorption site for pollutants. The proposed study will investigate the efficacy of GAC adsorption in the presence of nanomaterials. Three nanomaterials (titania, zero valent iron, and silica) at two concentration levels will be evaluated in the study.

The secondary objectives are:

- To determine the particle size distribution of nanoparticles by dynamic light scattering at different concentrations in nanopure water.

- To examine the interaction of $Fe_2O_3$, $TiO_2$, and $SiO_2$ with TCE in water, more specifically to examine the degree of adsorption of TCE on these materials.

- To conduct an adsorption isotherm study of TCE in the presence and absence of nanomaterials on GAC.

- To examine the efficacy of a GAC column in removing TCE in the

presence and absence of nanomaterials.

Further experiments will be conducted in the presence of 5 mg/L humic acid in order to more closely model natural water conditions, and to determine how NOM will impact the GAC application.

## 2.0 Literature Review

### 2.1 Environmental Nanotechnology

Nanotechnology involves the engineering of atomic-scale devices and systems. Due to seemingly endless possibilities, it is a field that experts believe will become one of the major industries of the 21st century (Sharpe, 2006). Scientists and engineers have been manipulating matter at the nanoscale to create nanoparticles, defined as objects between 1 to 100 nm in size. These nanoparticles are subsequently being used by industry in a multitude of commercial products, including food, sunscreen, cosmetics, sporting goods, washing machines, refrigerators, paint, and baby products (Allen, 2008). In 2005, a study showed that nanotechnologies were found in $30 billion worth of commercial goods. The same study predicts that this figure will increase to $2.6 trillion by 2014 (Holman et al. 2006). Environmental applications of nanotechnology has emerged as a key area of interest for researchers as a field known as environmental nanotechnology. Although this field has great potential in areas such as water treatment and pollution detection and prevention, there are many concerns that nano-scale objects and devices create new risks to human health and the environment (Sharpe, 2006). Therefore it is necessary to identify these impacts in the early stages of nanotechnology, rather than after this technology has been widely diffused (Guzman et al., 2006).

Health concerns for nanoparticles relate primarily to free, man-made nanostructures rather that ones fixed to a material (Nanoscience and nanotechnologies: opportunities and uncertainties, 2004). Nanoparticles that are not anchored to another material create a higher potential for exposure through inhalation, ingestion, and skin penetration, which would likely occur through environmental contamination, direct

application or ingestion of a specific product or food item, or through occupational exposure to workers (Nanomaterials – A risk to health at work 2004). The potential for exposure is problematic because little is understood about the toxicity of nanomaterials. Many experts believe that certain nanoparticles possess the ability to cross the cell barrier as well as the blood-brain barrier. Toxicity studies of metal and metal oxides (Cu, Co, $TiO_2$, and $SiO_2$ have been shown to have inflammatory effects on cells (Rahman et al., 2002). In fact, $TiO_2$ nanoparticulates have been shown to induce deoxyribonucleic acid (DNA) damage and chromosomal aberrations (Nakagawa, 1997). Carbon nanotubes, used in electrical circuits and other areas of nanotechnology, have been found to be cytotoxic and may lead to cancer (Jia et al., 2005). Research suggests that in general, many of the manufactured nanoparticles are more toxic per unit mass than their bulk counterparts (Sharpe, 2006). Overall, knowledge of nanomaterial toxicity has many gaps and further research is imperative.

Engineered nanomaterials may not only pose a risk to human health, but to the environment as well. The appearance of nanoparticles in the environment will likely come from several sources. The disposal or spillage of commercial products containing nanomaterials will inevitably lead to the presence of nanoparticles in the environment. The intentional release of nanomaterials, such as iron oxide, for environmental remediation will compound this problem (Hannah, 2008). The risk of nanomaterials in the environment, particularly drinking water sources, is assessed in this study.

Nanomaterials pose a risk to human health and the environment. However, if the health and safety concerns are addressed sufficiently, environmental nanotechnology could be used to create solutions to a wide range of environmental problems (Sharpe,

2006). In situ remediation of contaminants such as polychlorinated biphenyls (PCBs), organochlorine pesticides, and halogenated organic solvents could be facilitated through the use of bimetallic nanoparticles, such as iron/palladium or iron/silver (Sharpe, 2006). In addition, nanotubes have been shown as a "super-sorbent" material for dioxins. The unique properties of nanomaterials could also lead to a new wave of sensors capable of detecting pollutants at the molecular level. Finally, the use of nanoparticles in membranes, and as oxidants or adsorbents has the potential to significantly improve the efficiency of water treatment processes (Bottero et al., 2006).

Membrane technologies play many important roles in water treatment, ranging from particle removal and organic removal to desalination. The development of nanostructured membranes may yield membranes of greater selectivity and lower cost for water treatment (Bottero et al., 2006). Such nanoparticles as metal oxanes can be used to create nanostructured ceramic membranes, which are indefinitely stable both in solution and in the solid state (Bottero et al., 2006). Due to their high reactivity and surface area, nanomaterials can potentially be used as adsorbents in water and wastewater treatment. The most dominant research work involving nanoparticles as adsorption sites has dealt with using various forms of iron nanoparticles for arsenic adsorption (Bottero et al., 2006). Overall, the emerging field of environmental nanotechnology will lead to tremendous improvements in water and wastewater treatment.

## 2.2 Organic Pollutant Removal by Activated Carbon Adsorption

The Safe Drinking Water Act (SDWA) was passed by congress in 1974 as a result of public concerns of chemical contamination of drinking water sources. The SDWA

required the Environmental Protection Agency (EPA) to establish national standards for controlling the concentration of contaminants in drinking water. By this act, contaminants are defined as any physical, chemical, biological, or radiological substance or matter in water (Clark and Lykins, 1989). In 1986, amendments were made to the SDWA to include the control of volatile organic chemicals (VOCs) and pesticides in drinking water (Ram, 1990). The 1986 amendments to the SDWA required the EPA to set feasible maximum contaminant levels (MCLs) for 83 specific contaminants. The term "feasible" was defined as "with the use of the best technology, treatment techniques, or other means which the administrator finds available." Under these amendments, granular activated carbon was named a "feasible" technology for the control of synthetic organic contaminants (SOCs) (Ram, 1990). Thus the 1986 amendments to the SDWA created a surge in research and implementation of activated carbon treatment systems. Although activated carbon was initially used in the 1970's to treat drinking water for taste and odor causing compounds, it was implemented on a much larger scale in the 1980's for organics and pesticide treatment (Binnie, 2002).

Activated carbon is a highly adsorbent material derived from a diverse group of materials having a high carbon content. These materials include coconut shells, anthracite coal, peat, sawdust, lignite, and wood. A wide range of materials are used because each yield a type of activated carbon with different properties that have specific applications in water and gas phase adsorption (Faust and Aly, 1987). The term activation refers to the process in which the adsorptive properties of the source material are greatly enhanced and is usually classified as physical or chemical activation. One common activation process is a type of oxidation, which involves a reaction between the

carbon and oxidizing gases of steam, air, and carbon dioxide at very high temperatures (Faust and Aly, 1987). The end product of the activation process is a material having a highly porous and completely random imperfect structure which possesses pore sizes at molecular dimensions. Due to the porosity of this material, the surface area is extremely large, typically around 1000 $m^2/g$. In fact, activated carbon has the strongest physical adsorption forces or the highest volume of adsorbing porosity of any material known to mankind (Cheremisinoff, 2002).

Adsorption is the process where molecules are concentrated on the surface of the carbon. This process is caused by London Dispersion Forces, which are a type of Van der Waals Force that exists between molecules. This force is similar to the gravitational force between planets; however, London Dispersion Forces are very short-ranged (Cheremisinoff, 2002). These forces are also additive, meaning that the adsorption force is the sum of all interactions between all atoms (Cheremisinoff, 2002). Although activated carbon has the strongest physical adsorption forces of any material, it is not used for the removal of all contaminants in water. It is traditionally used for the removal of color, taste, and odor causing contaminants, as well as such organic compounds as benzene, trihalomethanes, and trichloroethylene. Activated carbon can also be used to remove a limited number of inorganic contaminats such as arsenic, mercury, iodine, and chromium (Cheremisinoff, 2002).

In general, organic contaminants are most effectively adsorbed by activated carbon. Organic compounds are composed of two basic elements, carbon and hydrogen. Because similar materials tend to associate, these compounds are most effectively removed by activated carbon. More specifically, organic compounds and activated

carbon are composed of similar elements; therefore, there is a stronger tendency for most organic molecules to associate with the activated carbon rather than staying dissolved in water (Cheremisinoff, 2002). This explains why in general, organic molecules having a low solubility are most strongly adsorbed.

In a water treatment facility, either powdered activated carbon (PAC) or GAC can be used in a variety of arrangements. When designing a system using PAC, careful consideration must be taken in selecting the PAC application point. The best location for the addition of PAC is at the head of the plant, either in the source water pipeline or in a basin for rapid mixing. Applying PAC at this point is ideal because it provides the longest contact time before the application of coagulants and other chemicals, which can interfere with adsorption rates (Brady, 1990). Typical PAC dosages range from 2 to 20 mg/L, but can go as high as 100 mg/L for severe taste and odor causing compounds. Another possible application point for PAC is directly prior to filtration. This will yield an efficient use of PAC for removing taste and odor causing compounds; however, some PAC may pass through filters and go into the distribution system. (Brady, 1990).

Unlike PAC, which is applied loosely to water in a treatment facility, GAC is fixed in an adsorber bed. There are three basic options for the location of the GAC application. The most common location for GAC beds is after the filtration process and prior to disinfection. At this location, GAC is used solely for the removal of dissolved organic compounds (Brady, 1990). Another option involves combining filtration and adsorption into a single treatment step. Finally, prefiltration adsorption is where the GAC beds are located at the head of the plant. This option; however, has limited applications and benefits (Brady, 1990). Once a location for GAC treatment has been

selected, several design factors must be evaluated. The first is the breakthrough of the bed, which can be defined as the point in which the effluent concentration of a contaminant exceeds the treatment objective (Brady, 1990). Other parameters, such as empty bed contact time (EBCT), flowrate, hydraulic loading rate, and carbon usage rate, can all be optimized to yield the most desirable breakthrough behavior. For example, a decrease in flowrate will yield a longer EBCT, which in turn will delay breakthrough and improve the carbon usage rate. However, decreasing the flowrate through a GAC system may require a larger or even multiple adsorber beds, which will increase cost. Therefore, all the aforementioned design parameters can be optimized to achieve the most ideal breakthrough behavior at the least cost.

Compared to sand and anthracite, activated carbon is an expensive filter media. As a result, it is usually cost-effective to regenerate and reuse spent GAC, which can be done on or off-site. On-site regeneration systems typically consist of a drying system for the spent carbon, a furnace, and a reactivation step (typically steam, thermal, or chemical) (Brady, 1990). On-site regeneration systems are very expensive and are only ideal for treatment facilities with high carbon usage rate. Off-site regeneration is similar to on-site regeneration, except the spent carbon is usually shipped back to the supplier for regeneration (Brady, 1990). Regenerated carbon may have lost some of its adsorptive capacity; therefore, is usually mixed with virgin carbon to optimize use.

Activated carbon is an ideal technology for the removal of organics and taste and odor causing compounds. One major limitation for this technology occurs during the competitive adsorption of NOM and organic pollutants. In the presence of NOM, the

removal efficiency of organic pollutants may decrease significantly due to several mechanisms described in the following section.

## 2.3 Impact of NOM on Micropollutant Adsorption

Activated carbon is one of the best available technologies for the simultaneous removal of micropollutants and NOM from drinking water. However, the adsorption of NOM can adversely affect the adsorption capacity and adsorption kinetics of many micropollutants such as organic compounds and pesticides. NOM is almost always present in drinking water sources at the mg/L level, which is much higher than trace contaminants that are usually at the ng/L to µg/L level (Quinlivan et al., 2005). Achieving a treatment objective for compounds such as SOC's and pesticides in the presence of NOM can be challenging because the impact of NOM on the adsorption of micropollutants depends on many different factors. The two most important mechanisms for the reduction in micropollutant adsorption are direct site competition and pore blockage. Adsorption kinetics are also important to understand because NOM will almost always adsorb before the micromolecules, which can lead to pore blockage. Furthermore, the pore size distribution (percentage of micropores, mesopores, and macropores) of the activated carbon is very important. For instance, the impact of NOM adsorption on micropollutants for activated carbons that have a large percentage of small micropores (<10Å) is usually more severe than for carbons that have larger micropores and a broader pore size distribution (Newcombe et al., 2002). Understanding how NOM will impact the adsorption of organic pollutants requires extensive research because the impact of NOM varies greatly depending on such factors as the type of carbon, NOM

molecular weight, and the target organic compound. Below are summaries of a few studies that illustrate the complexity of competitive adsorption.

A study was conducted in 2005 by Quinlivan et al. to determine how the physical and chemical characteristics of three ACF's and three GAC's impacted the simultaneous adsorption of NOM, TCE, and MTBE. This was accomplished by conducting adsorption isotherm experiments in the presence and absence of NOM as single solute systems of either TCE or MTBE. Isotherms were either conducted in ultrapure laboratory water or Sacramento-San Joaquin Delta water (SJDW), which had a DOC of 4.0 mg/L. Isotherm data was then described using the ideal adsorbed solution theory (IAST), and the fraction of NOM was represented by a single, hypothetical compound called the equivalent background compound (EBC). The results of this isotherm study were characterized in the pore structure effects and the surface chemistry effects of the various activated carbons used. It was shown that the surface chemistry of the activated carbons used had an impact of the adsorption of TCE and MTBE in the presence and absence of NOM. The extent of TCE and MTBE adsorption in the SJDW was greater for the more hydrophobic carbons and lesser for the hydrophilic carbons. This was attributed to the enhanced water adsorption onto the hydrophilic carbons that hindered TCE and MTBE adsorption. Nearly all of the carbons used in this work had very similar narrow pore size distributions (approximately 84% micropores, 16% mesopores). It was observed that micropollutant adsorption capacity decreased in adsorbents with larger micropores. This was due to pore blockage at the micropore entrance by the NOM. It was recommended by the authors in order to prevent pore blockage, the dominant micropore width should be approximately twice the diameter of the target adsorbate. This study shows the

importance of examining the predominant micropore size in relation to the size of the target micropollutant when selecting an activated carbon.

Another study was conducted in 2005 by Faur et al. to model the adsorption behavior of pesticides and metabolites (atrazine, deethylatrazine, deisopropylatrazine, and simazine) onto an activated carbon fiber (ACF) having a broad pore size distribution (32% mesopore volume, 68% micropores). Single solute, as well as multi-component isotherms were conducted for all compounds in order to determine the impact of solubility on adsorption. In addition, isotherms for atrazine in the presence of NOM were conducted. These isotherms were conducted in raw Erdre River (France) water having a DOC of 18.2 mg/L. Surprisingly, the presence of NOM has no impact on the adsorption capacity of atrazine for the ACF used. Several reasons were given for this phenomenon. First, NOM was shown to be very weakly adsorbed onto this particular ACF; therefore, NOM adsorption does not disturb the adsorption of atrazine. Also, ACF's that are highly microporous have been shown to exhibit high levels of pore blockage by large molecular compounds. This ACF has a broad pore size distribution, which lessens the pore blockage phenomenon. The micropores of this ACF can be divided into primary (<0.8nm) and secondary (0.8 to 2.0 nm). The authors believe that the large mesopore volume of the ACF used in this study enables some NOM adsorption, but pore blockage is negligible because atrazine adsorption occurred in the primary and secondary micropores.

Another study conducted in 2003 by Matsui et al. involved conducting adsorption isotherm experiments using two strongly adsorbing SOC's (simazine and simetryn) and one weakly adsorbing SOC (asulam) in the presence and absence of NOM. A wood

based PAC and a coal based PAC, both manufactured by Calgon Inc., were used in the isotherm experiments. This study found that the extent of adsorption for all three compounds was independent of initial concentration. Adsorption capacity of all three compounds was shown to decrease for isotherms conducted in the presence of NOM. However, there was no significant change in the pore diffusion coefficients between isotherms conducted in the presence and absence of NOM. Therefore, NOM competed with the three SOC's for adsorption sites, but did not block or fill micropores where adsorption was taking place. TOC of the natural river water used in each isotherm experiment ranged from 4 to 9 mg/L. The authors contend that this NOM loading was not severe enough to block the micropores of the PAC and thus hinder the internal diffusion of the three contaminants.

The last study discussed in this section was performed by Ebie et al. in 2001. This research endeavor examines only the impact of pore size distribution on adsorption. In this research, the impact of NOM on the adsorption of four agricultural chemicals (dichiorvos, fenobucarb, fenitrothion, and thiobencarb) was studied for three coal based carbons, each having a different pore structure. This task was completed by conducting batch adsorption isotherm experiments in the presence and absence of NOM. Adsorption of all four agricultural chemicals was shown to decrease dramatically in the presence of NOM for all three activated carbons. It was also shown that pore blockage by the NOM accounted for 10-99% of the total capacity reductions of the four micropollutants. Therefore, pore blockage, rather than direct site competition, was the most important mechanism for the adsorption capacity reductions of all the compounds studied. By correlating the competitive adsorption of NOM and the micropollutants to the pore size

distribution showed that the volume percentage of the carbon with pore sizes below 30 Å controlled the competition effect. For all four micropollutants, Carbon A showed the greatest reduction in adsorptive capacity in the presence of NOM. This is due to the high percentage of micropores this carbon possessed in the 0-15 & 0-30 Å range. Therefore, the authors suggest that using activated carbons that have a broader pore size distribution and a larger percentage of pores above 30 Å can lessen the impact of pore blockage by NOM. In turn, this will lead to a greater extent of adsorption of these four micropollutants.

The above studies sufficiently illustrate the complexity of multi-component systems containing organic pollutants and NOM. The reduction in adsorptive capacity of the organic micropollutants depends mostly on the factors listed below:

- Carbon pore size distribution
- Micropore size
- Surface chemistry characteristics
- Molecular size and concentration level of NOM
- Kinetic size of the micropollutant
- Pore blockage vs. direct site competition

## 2.4 Trichloroethylene

Trichloroethylene (TCE) is a contaminant commonly found in ground and surface water. Major environmental releases of TCE are due to air emissions from metal degreasing plants. Other releases come from metal finishing, electrical component, paint

and ink formulation, and rubber processing wastewaters. The production and use of TCE in the United States has increased significantly since 1981. In 1991, 320 million pounds of trichloroethylene were produced in the United States (National Primary Drinking Water Regulations). Vapor degreasing of metal parts and some textiles accounts for 80% of TCE use. An estimated 10 percent of production in the U.S. is exported.

TCE leaches readily through soil with low potential for adsorption to sediments. Mobility is considered high to very high in soil. The relatively high Henry's Law Constant indicates rapid evaporation from surface water. TCE biodegrades very slowly in soils and ground water. The properties of TCE are:

- Melting Point - -73ºC
- Specific Gravity at 20ºC – 1.465
- Boiling Point – 87ºC
- Water Solubility at 25ºC – 1 gram/Liter of Water
- Vapor Pressure at 20ºC – 57.8 mm Hg
- Henry's Law Constant – 0.01 atm-cu m/mole

The U.S.EPA has classified TCE as a human carcinogen and has issued a drinking water MCL of 5 μg/L.

In-situ removal of dissolved TCE from drinking water sources can be achieved through several water treatment processes such as pump and treat systems, permanganate oxidation, air-sparging, bio-sparging, dual phase vacuum extraction, low permeability

barrier walls, and reactive barriers (Carey, 2002). Ex-situ chemical methods for treatment of dissolved TCE in drinking water sources include advanced oxidation processes (ozone, hydrogen peroxide, and potassium permanganate) and dehalogenation with zero-valent iron. Bioremediation with aerobic and anaerobic bacteria involving oxidation, reduction or a combination of both mechanisms has been shown to be effective in the degradation of dissolved TCE. Pulsed corona discharge has also been effective (Shani, 2001). Ex-situ physical methods could be achieved through GAC adsorption.

## 2.5 Nanoparticles as Adsorption Sites

Nanotechnology is defined as a branch of engineering that deals with creating objects smaller than 100 nm in dimension (Wiesner, 2006). It has been shown in previous studies that commercially available nanomaterials have the capacity to adsorb various contaminants, both organic and inorganic. Due to their small size, nanoparticles have very high surface areas compared with their bulk counterparts. Because surface area is a key parameter in chemical reactions, particles tend to be more reactive at the nano-scale level (Sharpe, 2006). Nanoparticles also exhibit higher chemical reactivity due to unusual crystal-lattice order and surface chemistry that result in usefulness for adsorption of toxic species (Apblett, 2006). Nanomaterials also behave differently than their bulk counterparts because the relative importance of physical laws shifts and quantum effects start to become more dominant, especially for sizes less than 20 nm (Sharpe, 2006). Nanoparticles used in water treatment are generally anchored to a substrate or coated onto a larger particle in a controlled treatment scenario where the

nanomaterials do not exit the system. In turn, nanoparticles that are present in surface water and drinking water can become a potential health hazard. Since nanoparticles take a very long time to settle, they are likely to be carried by water, along with the hazardous adsorbates, to the consumer (Senftle et al., 2007).

Zheng et al. (2007) found that under optimum pH 4.0, the adsorptive capacity of titania nanoparticles for p-nitrophenol was 43%. When titania nanoparticles were modified with salicylic acid (SA) and 5-sulfosalicylic acid using a surface modification technique, adsorption capacity improved to 89% and 94%, respectively. In a study conducted by Liu & Xiao (2007), adsorption of polyethylene oxide (PEO) onto the surface of 10 nm silica particles was examined. In aqueous suspension, the silica nanoparticles were shown to adsorb PEO macromolecules through strong hydrogen bonding between OH-groups provided by silica and the ether oxygen groups of PEO. The removal of arsenate by ion-exchange media modified with iron hydroxide nanoparticles was studied by Hristovski et al. (2007). Through isotherm experiments it was shown that arsenate adsorption significantly increased when the ion-exchange media was impregnated with iron hydroxide nanomaterials (>10% of dry weight). Nanoparticles have also been show to have a high adsorptive capacity for metals. Cadmium removal from a simulated industrial wastewater using sol-gel structured $SiO_2$ and $Al_2O_3$ nanoparticles was examined by Pacheco et al. (2006). It was found that $SiO_2$ particles surrounded by $Al_2O_3$ nanoparticles could reduce cadmium concentrations from 140 ppm to <5 ppb by ion adsorption.

No studies to date have attempted to quantitatively describe the adsorption behavior of $TiO_2$, $SiO_2$, and $Fe_2O_3$ nanoparticles for TCE. In this study, we first

determine the particle size distribution in water of the three target nanomaterials. By conducting adsorption isotherm experiments in the presence and absence of these nanomaterials and NOM, we determine how these three nanomaterials impact the activated carbon adsorption of TCE. In this study, we also quantify the extent of TCE adsorption onto the three nanomaterials considered.

## 3.0 Experimental and Analytical Methodology

### 3.1 Materials

#### 3.1.1 Adsorbents

Norit E Supra USP Powdered Activated Carbon (Norit Americas, Inc.) was used for all adsorption isotherm experiments. This is a peat-based activated carbon with an Iodine number of 850, a Molasses number of 240, a BET surface area of 900 $m^2/g$, and an apparent density of 0.36 g/mL. 95% by weight of the PAC used had a diameter between 10 and 90 μm. Filtrasorb 400® (F-400) granular activated carbon was used for all column experiments. The F-400 was sieved to a particle diameter range of 0.841 to 1.19 mm. Prior to experimental use, both activated carbons were oven dried at 105° to constant weight, and stored in a desiccator until use.

#### 3.1.2 Nanomaterials

Three types of commercially available nanomaterials were used: $TiO_2$, $Fe_2O_3$, and $SiO_2$. A solution containing 20 nm $SiO_2$ was obtained from Alfa Aesar (Ward Hill, Massachusetts) as a 30% solution in ethylene glycol, as a colloidal dispersion. A solution containing 4 nm $SiO_2$ was also obtained from Alfa Aesar as a 15% solution in water, as a colloidal dispersion. $TiO_2$ nanopowder at a 30 nm particle size was obtained from Degussa Corporation (Dusseldorf, Germany) (product number: P25). $Fe_2O_3$ industrial APS powder at a particle size range of 20 to 40 nm was obtained from Alfa Aesar.

### 3.1.3 Adsorbates

TCE (Sigma-Aldrich; St. Louis, Missouri) at 99.9±% purity was used in this study. TCE is a common organic pollutant, with the molecular formula $C_2HCl_3$. All TCE standards were prepared in methanol. However, methanol concentrations in isotherm experiments were at or below 0.1%. Based on previous studies, no co-solvent effects are observed at this level (Quinlivan et al., 2005). Humic acid salt (Fluka; Milwaukee, Wisconsin) was used at a concentration of 5 mg/L to represent NOM in isotherm experiments. Model compounds such as fulvic or humic acid are often used in isotherm studies because they are projected to be responsible for most of the reactivity of NOM (Kilduff and Karanfil, 2002).

### 3.1.4 Water

All solutions analyzed for PSD or used in adsorption isotherm experiments were prepared in nanopure water having a resistivity greater than 18.0 Mega-Ohms per centimeter (MΩ-cm) and a total organic carbon (TOC) concentration less than 1.0 ppb. All water was autoclaved for 35 minutes at 121°C. Autoclaved water was then buffered to the desired pH. Solutions were buffered to a pH of 7.0±0.2 with 0.001M $KH_2PO_4$, and adjusted using 10N NaOH. Acidic solutions were buffered to a pH of 3.5±0.2 with 0.001M formic acid. Water for the GAC column experiments was prepared this way, except it was not autoclaved due to the large volume of water required for the breakthrough experiments.

### 3.1.5 Glassware and Analytical Instruments

250 ml Qorpak Amber Boston Bottles with Teflon (TFE)–Lined Closures (catalogue number: 03-320-4C) from Fisher Scientific were used in all adsorption isotherm experiments. In addition, 250 ml Qorpak Clear Boston Rounds with TFE Lined Closures (catalogue number: 03-326-3G) from Fisher Scientific were used for measuring particle size distribution. Columns of varying length and diameter obtained from ACE Glass were used for the column study. Chemdurance L/S 16 Precision Pump Tubing (Cat.# K-06432-16), along with two 12 gallon pyrex containers were also used in the column study.

For analyzing PSD, two instruments were used. First, a Spectrex Laser Particle Counter Model PC-2000 located at U.C. was used to determine PSD changes over time. Next, a HIAC Laser Particle Counter Model 9703 located at the EPA T&E Facility was used to measure PSD before and after each adsorption isotherm experiment. Analysis of humic acid concentration was performed spectrophotometrically by using a UV-VIS spectrophotometer (Hach DR/4000U). TCE analysis was performed using an Archon 5100 Purge & Trap Autosampler connected to a Tekmar 3000 Purge & Trap Concentrator. The purge and trap unit is interfaced to a Hewlett Packard 6890 gas chromatograph (GC) equipped with a flame ionization detector (FID). An Agilent DB-WAX column (J&W 123-7063) (60 m x 320 μm inside diameter with 0.50 μm film thickness) was used.

## 3.2 Methods

### 3.2.1 Particle Size Distribution Analysis

In order to characterize the aggregation behavior of the three nanoparticles targeted in this study, PSD analysis as a function of time was performed to determine the diameter at which each nanoparticle aggregate exists in water. PSD analysis was performed at nanoparticle concentrations of 0.5 and 1.0 mg/L for both $TiO_2$ and $Fe_2O_3$, and at 5.0 and 10.0 mg/L for $SiO_2$ (4 and 20 nm $SiO_2$ solutions). PSD analysis for both $TiO_2$ and $SiO_2$ was performed at neutral pH. However, the pH was lowered to 3.5 ± 0.2 for dissolution of the $Fe_2O_3$ nanoparticles prior to PSD analysis. All solutions were placed in 250 mL clear glass bottles and PSD measurements were performed weekly. During the first phase of PSD analysis, all bottles were left stationary on the bench-top for up to six weeks. During the second phase of PSD analysis, $Fe_2O_3$ and $TiO_2$ bottles that were previously left stationary on the bench-top were permanently maintained in a rotary tumbler and measurements were taken weekly thereafter. Solutions were kept in a rotary tumbler to inhibit the settling of any suspended nanoparticles. For the third phase of PSD analysis, nanoparticle solutions identical to those above were prepared and immediately analyzed and placed in a rotary tumbler, where measurements were taken weekly thereafter. PSD analysis was performed using a Spectrex Model PC-2000 Laser Particle Counter which utilizes dynamic scattering of light to determine the number of particles (at each diameter, ranging from 1 to 16 μm) per volume of sample. For further information regarding PSD experiments, see the Standard Operating Procedure (SOP) in Appendix 3.

### 3.2.2 Adsorption Isotherm Experiments

Single solute adsorption isotherm experiments were conducted at a temperature of 22.0ºC ±1.0 using the bottle-point technique (each bottle represents one data point). 250 ml Qorpak amber boston bottles with TFE–lined closures were used in all isotherm experiments in order to minimize the interaction of light with the nanoparticles or TCE. In order to prepare each isotherm experiment, TCE was added to buffered water in order to achieve three initial concentrations, which ranged from 400 to 1800 μg/L for each experiment. Two concentration levels of nanomaterials were used in each experiment (0.5 and 1.0 mg/L for $Fe_2O_3$ and $TiO_2$, and 5.0 and 10.0 mg/L for $SiO_2$). Isotherms experiments containing $SiO_2$ or $TiO_2$ were conducted at neutral pH, while isotherms containing $Fe_2O_3$ were conducted at pH 3.5±0.2 so that the nanoparticles immediately dissolve into solution. The three initial TCE concentrations were used in order to confirm the experimental adsorption results by providing one isotherm adsorption correlation for each condition studied (presence/absence of nanomaterials). All isotherm experiments were repeated in the presence of NOM. For these experiments, humic acid was added to the prepared solutions at a concentration level of 5 mg/L and mixed thoroughly. Varying amounts of PAC (1-10 mg) were added to each bottle. Prior to each isotherm experiment, all bottles were placed in a 550°C oven for at least four hours to ensure no TCE remained adsorbed to the glass. At each TCE concentration level, three bottles contained no PAC and thus acted as blanks. All bottles were overfilled (leaving no headspace), capped, and placed in a rotary tumbler for two weeks in order to reach equilibrium. Two weeks has been demonstrated by many preliminary rate studies to be adequate time for equilibrium to occur. A two week equilibrium period was also used by

Kilduff et al. (1998) in conducting adsorption isotherms for TCE onto activated carbon. For further information regarding isotherm experiments, see the SOP in Appendix 2.

First, isotherm experiments were conducted in the absence of nanomaterials in order to provide a baseline for characterizing how the nanoparticles will impact TCE adsorption. Isotherms were then conducted in the presence of either $TiO_2$, $Fe_2O_3$, or $SiO_2$ in order to determine how each nanomaterial impacted adsorption of TCE. Finally, all experiments were repeated at a humic acid concentration of 5 mg/L.

### 3.2.3 GAC Column Studies

Breakthrough studies were conducted for TCE in nanopure water and $SiO_2$ in order to determine the efficacy of the GAC adsorber in the presence of nanomaterials. The experimental data will be tested against an adsorber model (AD-Design software will be used) to determine their predictability.

In order to conduct these breakthrough experiments, the column was first wet-packed with a bed of F400 GAC in between two beds of coarse sand that had been washed with 1 M nitric acid and baked at 550°C for 4 hours. A stainless steel screen was placed at both ends of the column and at the contact point between the sand and GAC. The column was then covered in order to keep light out and to minimize the possibility of biological activity within the column. Next, two 12 gallon pyrex containers were filled with nanopure water and buffered to the desired pH. Prior to the addition of TCE, buffered water was run through the column for 24 hours in order to remove any air bubbles from the system. Next, TCE was added to each jug for a concentration of 2.5 mg/L, and allowed to mix thoroughly. Both jugs were then sealed and supplied with a $N_2$

headspace in order to minimize the loss of TCE due to volatilization. Using a peristaltic pump, the TCE solution was continuously pumped through the system at a constant flowrate for the duration of the experiment. Influent and effluent samples were taken daily, then filtered, diluted and analyzed in the GC. Figure 3.1 shows the GAC adsorber setup used for all breakthrough experiments.

**Figure 3.1** GAC Adsorber setup at EPA T&E Facility

## 3.3 Sample Analysis

### 3.3.1 TCE Analysis

TCE analysis was performed by filtering samples through a 0.45 μm filter, diluting, then placing the sample into a 44 mL amber vial for GC analysis. As previously stated, a HP 6890 GC equipped with a Tekmar 3000 Purge and Trap Concentrator was

used in accordance with EPA Method 5030C. The GC oven temperature was maintained at 40 $^{o}$C for the first 5 minutes, ramped 3°C/min to 70°C, then ramped 18°C/min to 160°C and maintained for 4 minutes. The flow rate of the carrier gas (He) was set at 2.5 ml min-1. The detector makeup gas (He) flow rate was set at 30.0 ml min-1. The flame gases hydrogen and air flow rates were set at 35.0 ml min$^{-1}$ and 400.0 ml min$^{-1}$, respectively. Tetrachloroethane(PCE) was used as an internal standard at a concentration of 29 µg/L. The retention times for TCE and PCE were 11.9 min and 13.25 min, respectively. TCE concentrations were determined from the area response ratio of TCE to PCE. Quality control procedures for TCE analysis are outlined in Appendix 4.

### 3.3.2 Humic Acid Analysis

Samples were filtered through a 0.45 µm filter and placed in a quartz cuvette for analysis. Analysis of humic acid concentration was subsequently be performed by using a UV-VIS spectrophotometer (Hach DR/4000U). A wavelength range of 200 to 500 nm was scanned for determination of absorbance. The area under the wavelength vs. absorbance curve was then used to calculate humic acid concentration.

### 3.3.3 Particle Size Distribution Analysis

PSD analysis performed using the Laser Particle Counter (Model PC-2000) is outlined in Appendix 3. PSD measured using the HIAC Laser Particle Counter is conducted by first placing the sample into a 250 mL flask. The instrument then pulled 10 mL of the sample for each reading. Blanks of nanopure water were run prior to analysis of every sample.

### 3.4 Calculation Procedure of Experimental Samples

#### 3.4.1 TCE Concentration

10 point calibration curves were constructed using the GC prior to analysis of samples. TCE concentrations ranged from 5 to 375 µg/L for each calibration. The area response of TCE divided by the area response of PCE (internal standard) was plotted against the theoretical TCE concentration in order to obtain a linear relationship of TCE Area / PCE Area vs. TCE Concentration. Therefore, linear regression was performed and a trendline equation was obtained. After analysis of a sample, the TCE concentration was determined using the following formula:

*(Calibration Curve Slope) x (TCE Area ÷ PCE Area) = TCE Concentration (µg/L)*

#### 3.4.2 Humic Acid Concentration

A five point calibration curve was constructed using the UV/VIS spectrophotometer prior to analysis of samples. Humic acid concentrations ranged from 1 to 11 mg/L for each calibration. A wavelength range of 200 nm to 500 nm was scanned for each concentration and the absorbance values at each wavelength was recorded. The area of the wavelength vs. absorbance curve for each concentration level was calculated using the trapezoidal rule below:

*Area = ((Abs_200 + Abs_210)*10)/2 + ((Abs_210 + Abs_220)*10)/2 + ……..……+ ((Abs_490 + Abs_500)*10)/2*

These area values were then plotted against the humic acid concentrations of each calibration point and a linear relationship was obtained. Therefore, linear regression was performed and a trendline equation was obtained. Humic acid concentrations for each sample are determined by the following formula:

*(Calibration Trendline Slope) x ( Sample Area Value) = Humic Acid Conc. (mg/L)*

### 3.4.3 Adsorption Isotherm Calculations

For each adsorption isotherm bottle containing PAC, the mass of TCE adsorbed per milligram of PAC was calculated. First, the mass of TCE in each bottle was calculated using the following formula:

*(Equilibrium TCE Conc. ($C_e$ ,µg/L)) x 0.25 = µg TCE per Bottle*

The mass of TCE adsorbed was then calculated using the following formula:

*(Initial TCE Conc. (µg/L) x 0.25) – (µg TCE per Bottle) = µg TCE Adsorbed*

The mass of TCE adsorbed for each bottle was divided by the amount of PAC in that bottle to determine the µg of TCE adsorbed per mg of PAC ($Q_e$). $C_e$ vs. $Q_e$ logarithmic plots were constructed for each adsorption isotherm experiment. Trendlines of these plots were found using linear regression. Modeling of TCE adsorption equilibrium data was performed using the Freundlich equation. This empirical model is

widely used in water treatment and satisfactorily describes adsorption equilibria of organics and inorganics onto a wide variety of adsorbents, including activated carbon (Otake et al.; 2004). The Freundlich equation is written:

$$Q_e = K * C_e^{1/n},$$

where $Q_e$ is the amount of TCE adsorbed (per PAC mass), $C_e$ is the equilibrium aqueous phase TCE concentration, K is considered a capacity parameter that expresses the extent of uptake corresponding to a value of $C_e$, and 1/n is a dimensionless parameter related to the site energy distribution (Kilduff and Karanfil, 2002).

### 3.4.4 GAC Column Calculations

Influent and effluent TCE concentrations were analyzed in order to plot ($C/C_o$) with time. This allowed us to measure the adsorptive capacity of the GAC being used. A simple mass balance equation was used to determine the mass of TCE adsorbed onto the GAC. Changes in breakthrough behavior between the experiment conducted in the presence of $SiO_2$ and in the absence of $SiO_2$ were examined.

## 4.0 Particle Size Distribution Experimental Results

### 4.1 Particle Size Distrubution

Prior to conducting the adsorption isotherm experiments, it was necessary to characterize the size distribution of the three nanomaterials studied. It was important to understand how nanoparticle aggregates behave in water because it is understood that nanoparticle aggregates have a higher adsorptive capacity for various compounds than the nanoparticles themselves. The objective of this part of the study was to determine whether $SiO_2$, $TiO_2$, and $Fe_2O_3$ nanomaterials will form aggregates larger than 1 μm in diameter, and whether these aggregates will increase in size with time. Nanoparticle solutions were evaluated under three conditions. For the first part of the PSD study, solutions were left stationary on the bench-top in between weekly measurements. For the second phase of this study, solutions that were previously left on the bench-top were permanently kept in a rotary tumbler in between weekly measurements. For the final phase of this study, new nanoparticle solutions were made and these bottles were immediately placed in a rotary tumbler and kept there in between weekly PSD measurements. The second and third phases of the PSD experiments were performed in order keep the nanoparticle aggregates in suspension and to determine if constant agitation of the solution would cause aggregates to increase in size. The results of these experiments are given in the following sections.

## 4.2 Particle Size Distribution for $SiO_2$

Particle size distribution for 5.0 and 10.0 mg/L $SiO_2$ in water was analyzed according to the method described in the previous chapter. PSD was analyzed for both the 4 and 20 nm diameter $SiO_2$ solutions over the duration of six weeks. During the first four weeks of this period, all of the $SiO_2$ bottles were covered and left on the bench top between PSD measurements. During the last two weeks of this six week period, all bottles were permanently maintained in a rotary tumbler. During this six week period, no particle counts greater than 1 μm were registered for both the 4 and 20 nm $SiO_2$ at both concentration levels. From this we can infer that no aggregation of nanoparticles is taking place for the 4 and 20 nm $SiO_2$. One explanation for the apparent lack of aggregation is that both sizes of $SiO_2$ were obtained as colloidal dispersions in solution, whereas the $TiO_2$ and $Fe_2O_3$ were obtained as nanopowders. Since no readings were registered for the $SiO_2$ solutions under both these conditions, it was not necessary to prepare a new set of solutions for the third phase of the PSD study.

## 4.3 Particle Size Distribution for $TiO_2$

The first set of $TiO_2$ nanoparticle solutions were analyzed for a period of nine weeks. For the first four weeks of this eight week period, the bottles were covered and left on the bench top in between PSD measurements (See Figures 4.1 and 4.2). For the final five weeks of this period, these bottles were continuously tumbled (See Figures 4.3 and 4.4) In Figures 1 and 2, we see a shift to the left in the most abundant particle sizes at both concentration levels, which translates into smaller particles being detected. We can infer that the suspended particles were actually settling out of solution, which was

visually seen. Therefore, these particles were not accounted for by the laser particle counter.

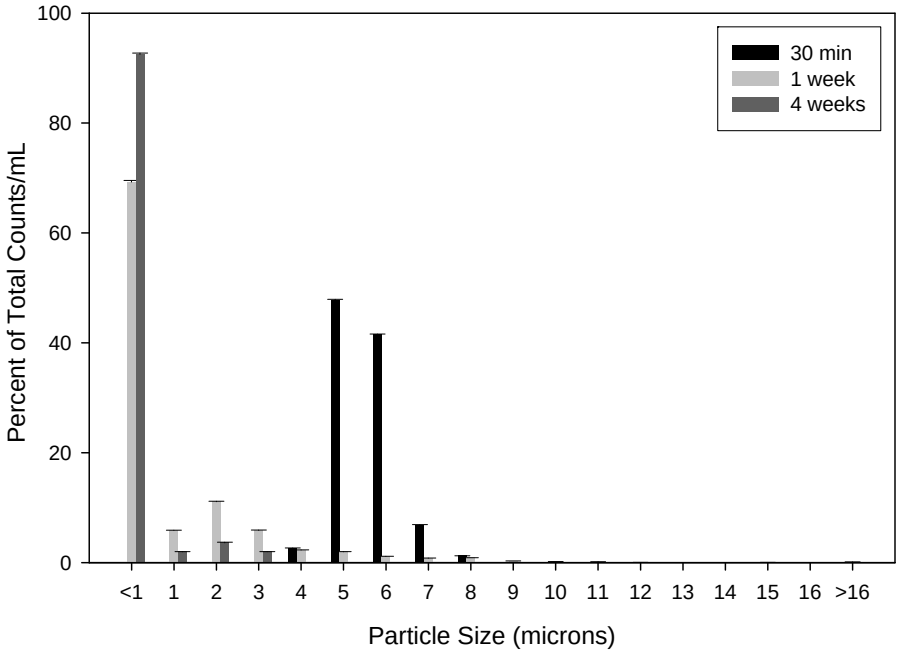


*No readings were registered for weeks 2 & 3.

**Figure 4.1** Particle size distribution of 0.5 mg/L $TiO_2$ solutions left stationary of bench-top.

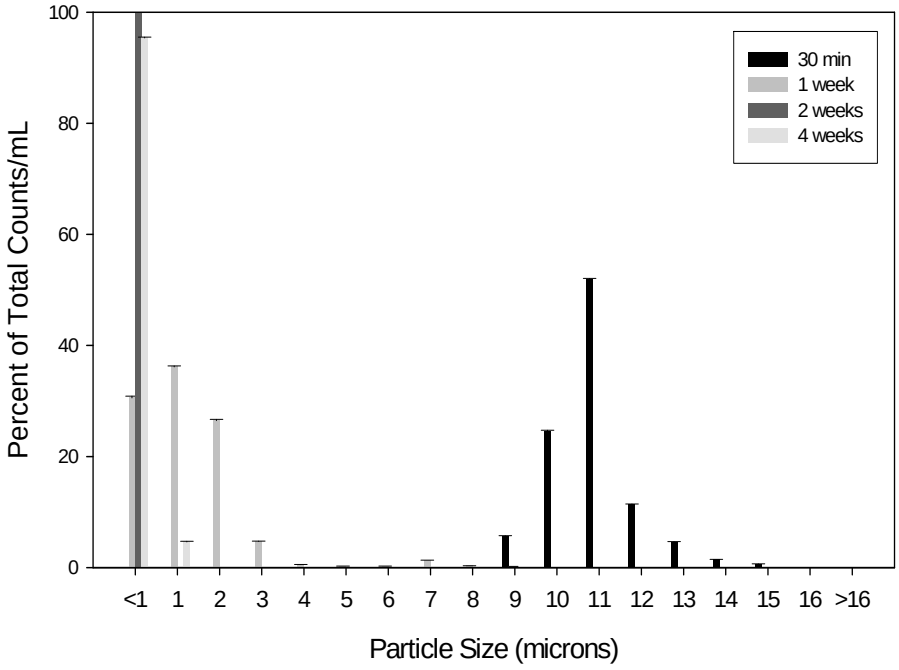


*No readings were registered for week 3.

**Figure 4.2** Particle size distribution of 1.0 mg/L $TiO_2$ solutions left stationary of bench-top.

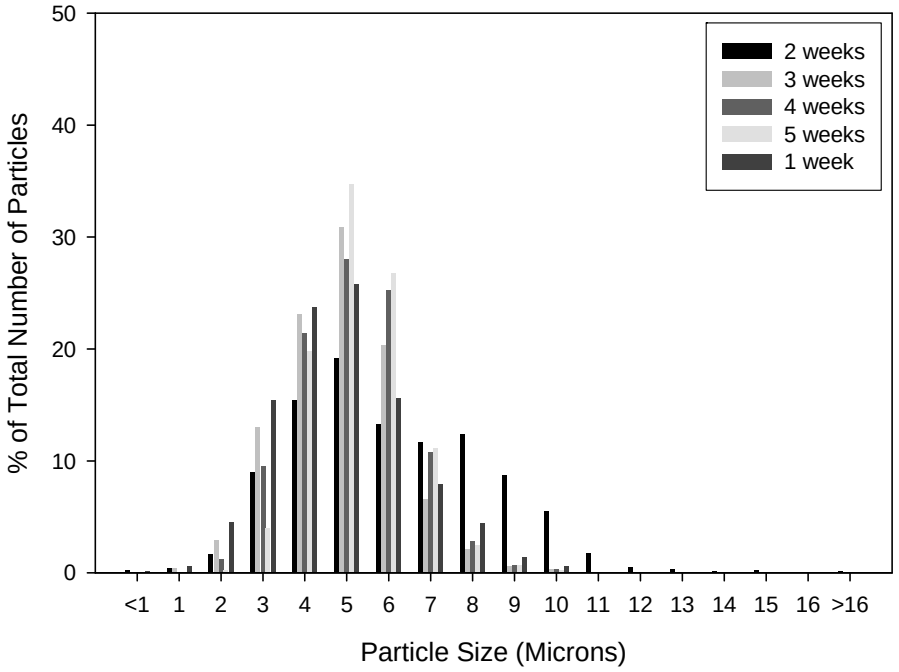


**Figure 4.3** Particle size distribution for 0.5 mg/L $TiO_2$ solutions placed in a rotary tumbler.

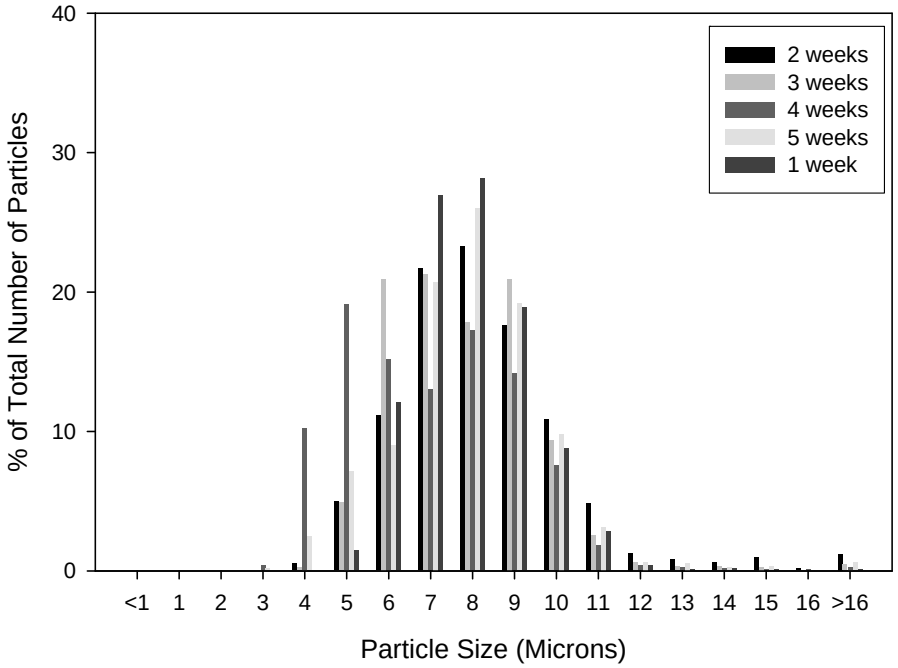


**Figure 4.4** Particle size distribution for 1.0 mg/L $TiO_2$ placed in a rotary tumbler.

During the last four weeks of analysis when the bottles were being continuously tumbled, as shown in Figures 4.3 and 4.4, we see a consistent Gaussian-shaped size distribution for both the 0.5 and 1.0 mg/L level. We can infer that adequate tumbling was provided to keep the particles suspended in solution. At the 0.5 mg/L level in Figure 4.3, the mean diameter is around 5 μm. At the 1.0 mg/L level in Figure 4.4, the mean diameter is around 8 μm. This shows that larger aggregates were formed at the higher concentration level. Figures 4.3 and 4.4 also show that the size distribution remains consistent with time; therefore under these conditions, $TiO_2$ aggregates stabilized quickly in water at both concentration levels and did not grow with time.

A second set of bottles were prepared for $TiO_2$ at the same concentrations and pH levels as above. PSD measurements for both these $TiO_2$ bottles were taken weekly for a period of 6 weeks. Unlike the previous sets of bottles, these bottles were continuously

tumbled from the time that the solutions were prepared, thus not allowing the nanoparticles to settle out of the solution. The data in Figures 4.5, 4.6, 4.7, 4.8, and 4.9 show that the size distribution on $TiO_2$ particles remains consistent with time. However, at both the 1.0 mg/L and 0.5 mg/L $TiO_2$ level, we see a larger aggregate than measured in the previous experiments where the bottles had been left on the bench-top then placed in the tumbler. At the 1.0 mg/L level, the mean diameter increased from 8 μm to approximately 11 μm. At the 0.5 mg/L level, the mean diameter increased from 5 μm to approximately 8 μm. This increase in particle size is likely due to the fact that the nanoparticles in the second set of solutions were not allowed to settle out of solution. From the plots we can infer that for both concentration levels of $TiO_2$ no further aggregation occurs beyond the initial aggregate formation that occurs when the nanomaterials are placed in water.

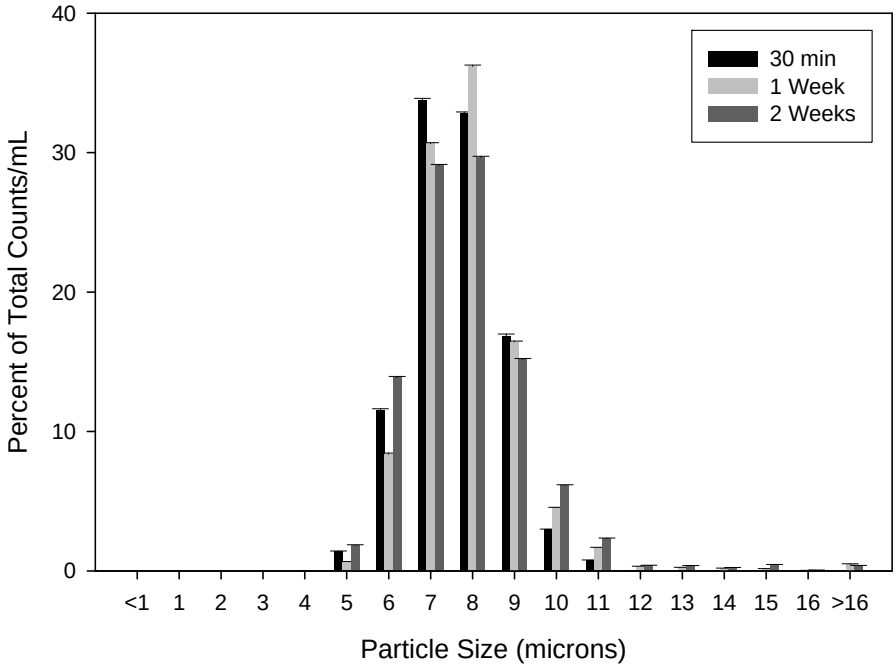


**Figure 4.5** Particle size distribution for 0.5 mg/L $TiO_2$ solutions permanently maintained in a rotary tumbler.

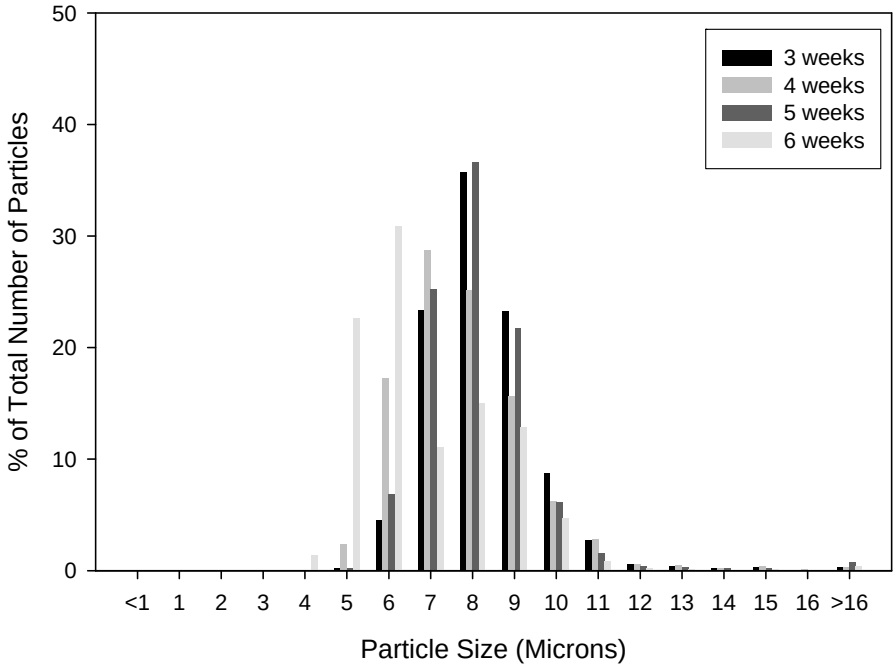


**Figure 4.6** Particle size distribution for 0.5 mg/L $TiO_2$ solutions permanently maintained in a rotary tumbler (Represents a continuation of data in Figure 4.5).

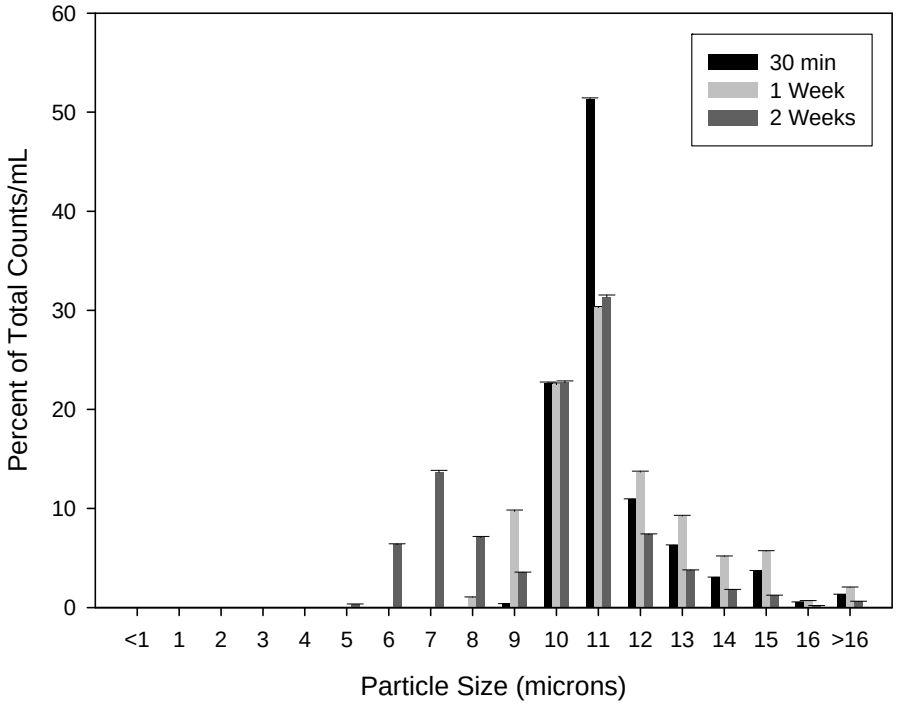


**Figure 4.7** Particle size distribution for 1.0 mg/L $TiO_2$ solutions permanently maintained in a rotary tumbler.

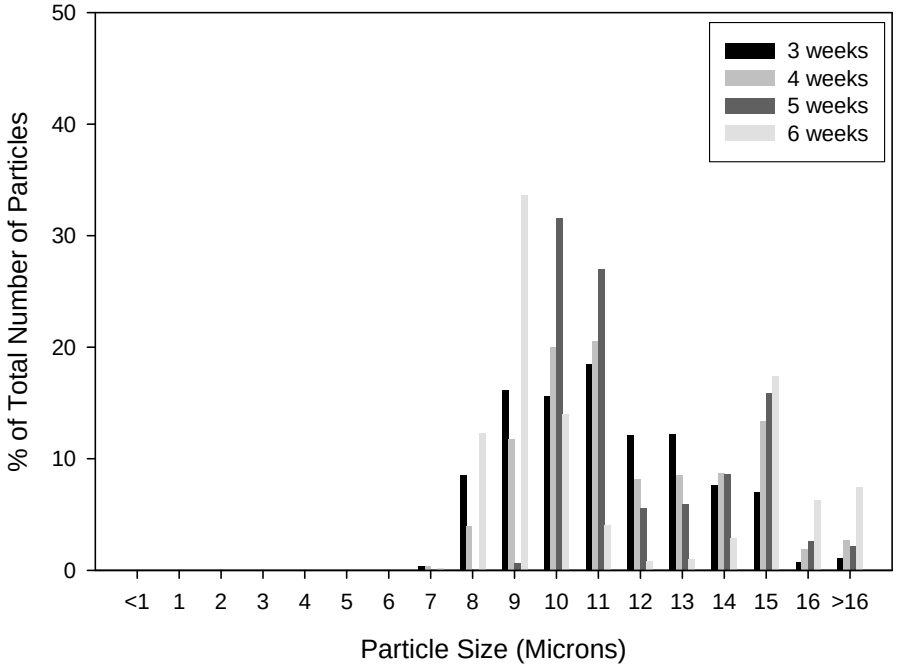


**Figure 4.8** Particle size distribution for 1.0 mg/L $TiO_2$ solutions permanently maintained in a rotary tumbler (Represents a continuation of data in Figure 4.7).

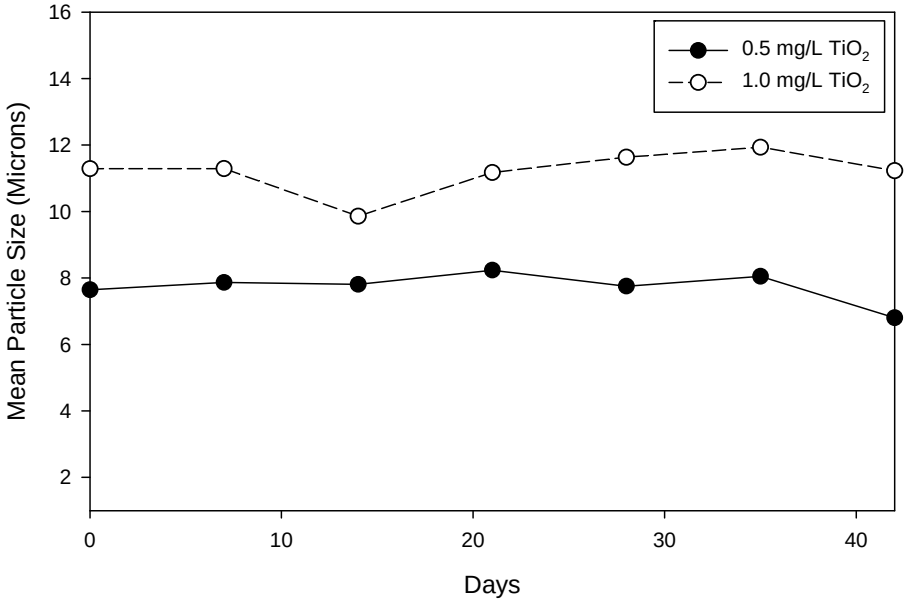


**Figure 4.9** Mean particle diameter for 0.5 & 1.0 mg/L $TiO_2$ solutions permanently maintained in a rotary tumbler.

### 4.4 Particle Size Distribution for $Fe_2O_3$

The first set of $Fe_2O_3$ solutions were analyzed over a ten week period. For the first four weeks of this ten week period, the bottles were covered and left on the bench top between PSD measurements (See Figures 4.10 and 4.11). For the final six weeks of this period, the bottles were continuously tumbled (See Figures 4.12, 4.13, 4.14, and 4.15) From the plots, we see a decrease in particle size during the first three weeks of analysis. Similar to the above phenomenon that occurred for the $TiO_2$ solutions, we can infer that the suspended particles were settling out of solution. During the last seven weeks of analysis when the bottles were being continuously tumbled, we see a consistent size distribution for both concentration levels. We can infer that adequate tumbling was provided to keep the particles suspended in solution. Unlike the aforementioned $TiO_2$ solutions, there was not a higher degree of aggregation of particles for the 1.0 mg/L

$Fe_2O_3$ versus the 0.5 mg/L $Fe_2O_3$. In addition, neither of the $Fe_2O_3$ concentration levels showed the Gaussian distribution that the $TiO_2$ solutions displayed within the 1 to 16 μm size range.

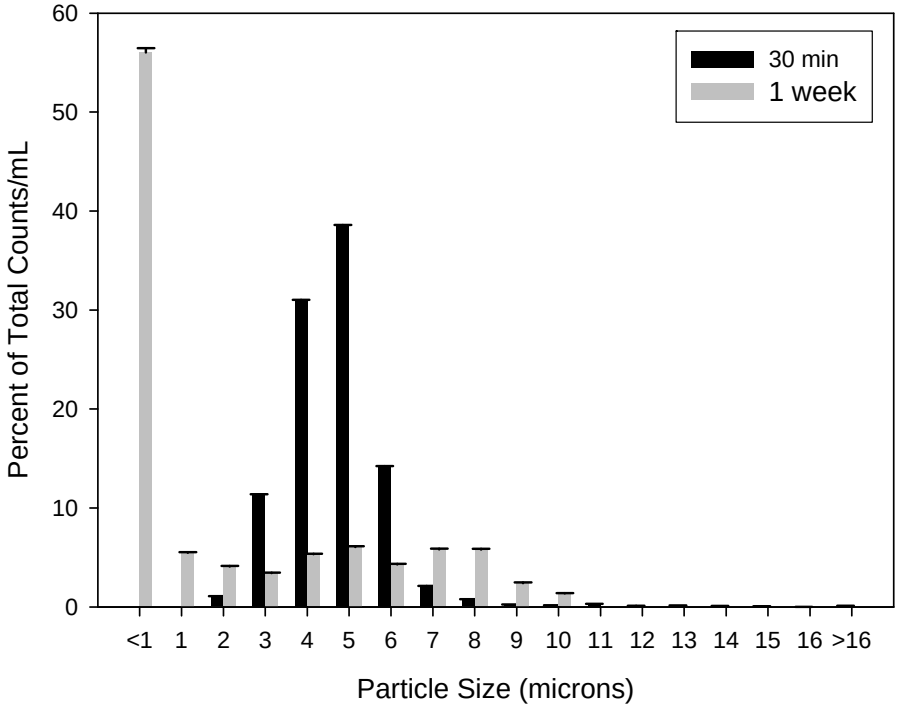


*No readings were registered for weeks 2 & 3.

**Figure 4.10** Particle size distribution of 0.5 mg/L $Fe_2O_3$ solutions left stationary on bench-top.

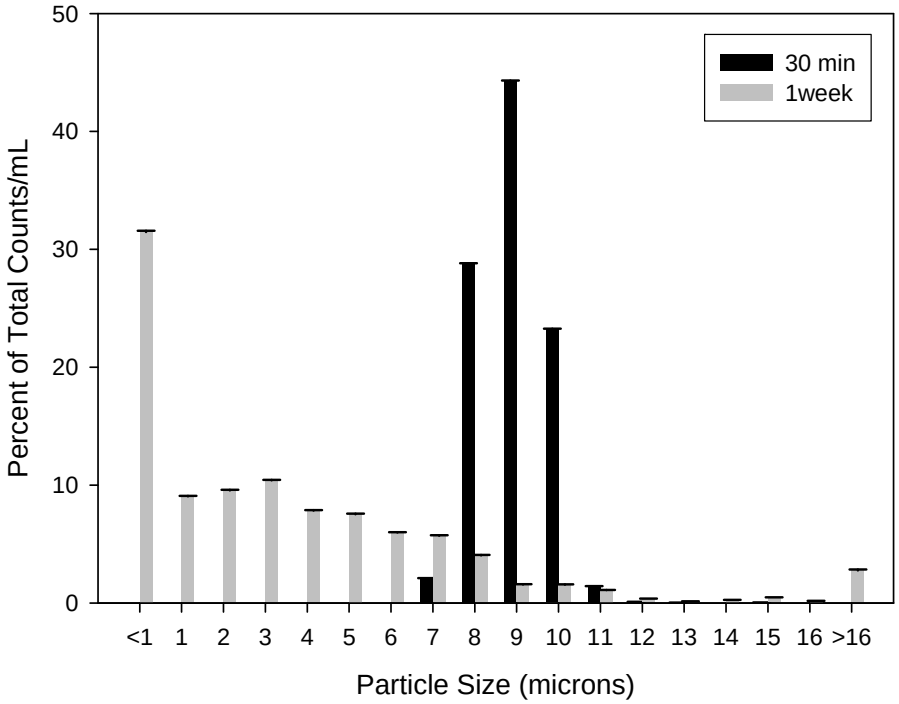


*No readings were registered for weeks 2 & 3.

**Figure 4.11** Particle size distribution for 1.0 mg/L $Fe_2O_3$ solutions left stationary on bench-top.

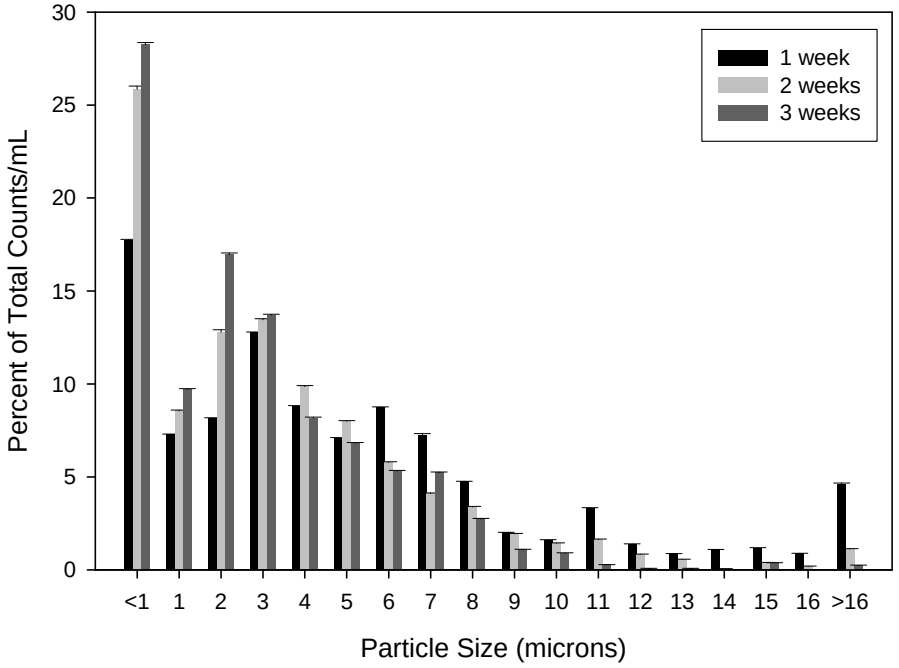


**Figure 4.12** Particle size distribution for 0.5 mg/L $Fe_2O_3$ solutions placed in a rotary tumbler.

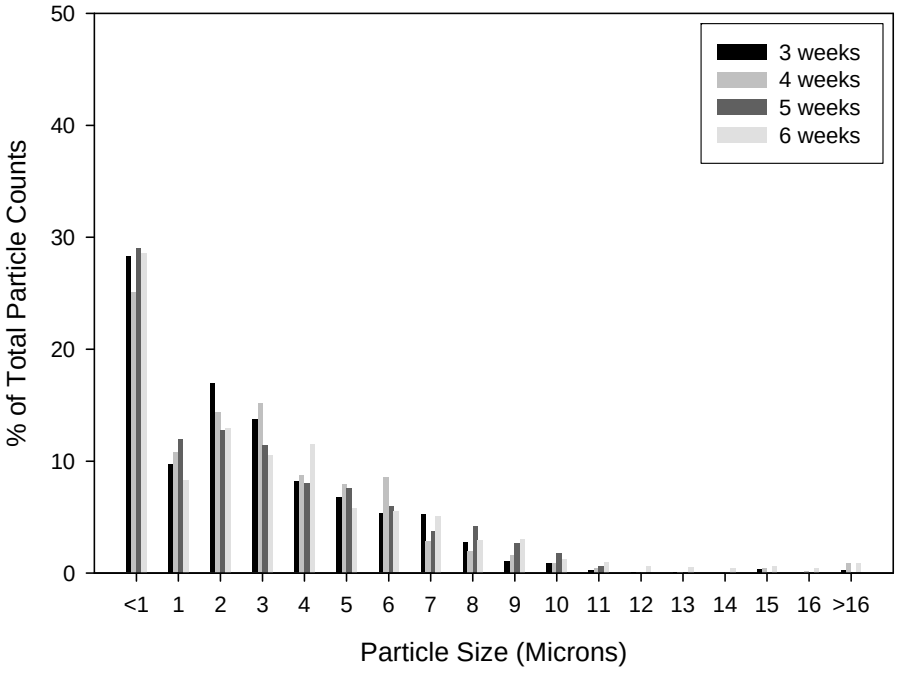


**Figure 4.13** Particle size distribution for 0.5 mg/L $Fe_2O_3$ solutions placed in a rotary tumbler (Represents a continuation of data in Figure 4.12).

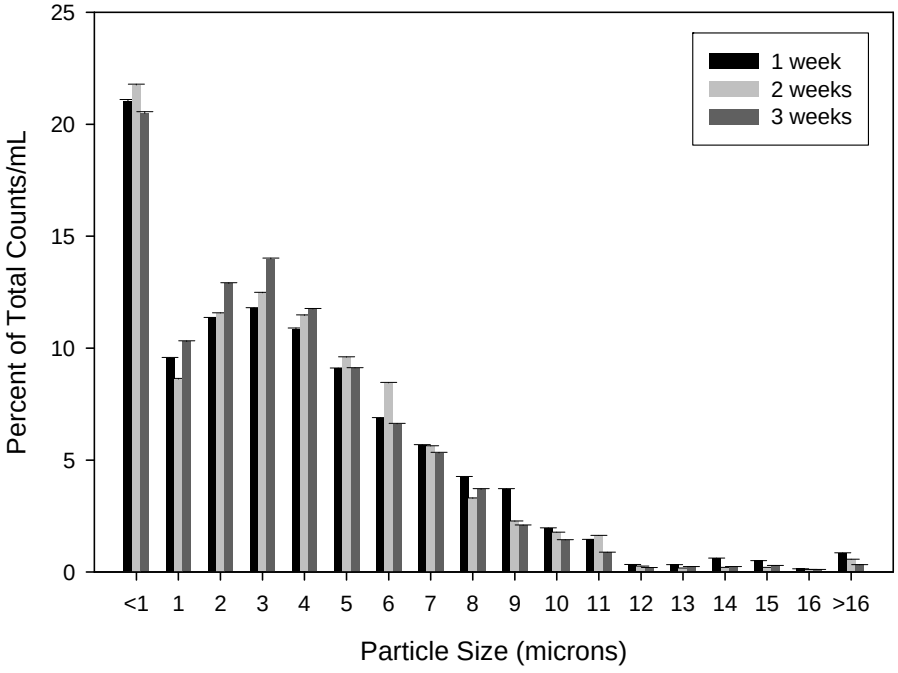


**Figure 4.14** Particle size distribution for 1.0 mg/L $Fe_2O_3$ solutions placed in a rotary tumbler.

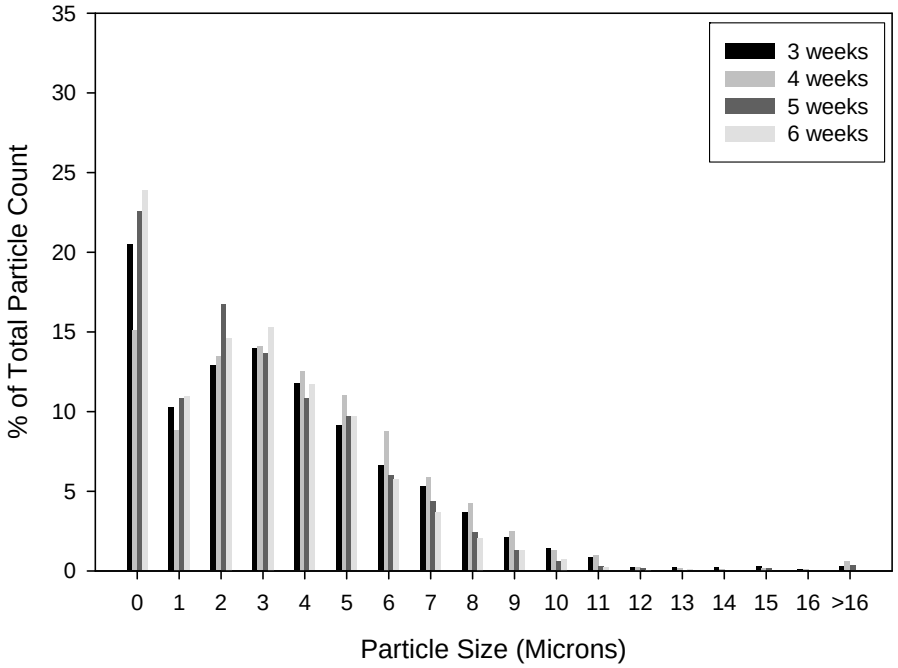


**Figure 4.15** Particle size distribution for 1.0 mg/L $Fe_2O_3$ solutions placed in a rotary tumbler (Represents a continuation of data in Figure 4.14).

A second set of solutions were prepared for $Fe_2O_3$ at the same concentrations and pH levels as above. PSD measurements for $Fe_2O_3$ solutions were taken weekly for a period of 6 weeks. Unlike the previous sets of bottles, these bottles were continuously tumbled from the time that the solutions were prepared, thus not allowing the nanoparticles to settle out of the solution. The data in Figures 4.16, 4.17, 4.18, and 4.19 shows that there is no significant aggregation of iron oxide particles with time, and size distribution was nearly identical to that shown in Figures 4.12 through 4.15. At the 30 minute point for both the 0.5 mg/L and 1.0 mg/L levels shown in Figure 4.16 and Figure 4.18, a much larger particle size was detected. This phenomenon was likely due to the fact that the PSD readings were taken too quickly after the solutions were prepared. Therefore, 30 minutes was not adequate time for the $Fe_2O_3$ particles to fully mix and

dissolve in solution. The same phenomenon can be observed in Figures 4.10 and 4.11. From this data we can infer that for both concentration levels of $Fe_2O_3$, no further aggregation occurs beyond the initial aggregate formation that occurs when the nanomaterials are placed in water.

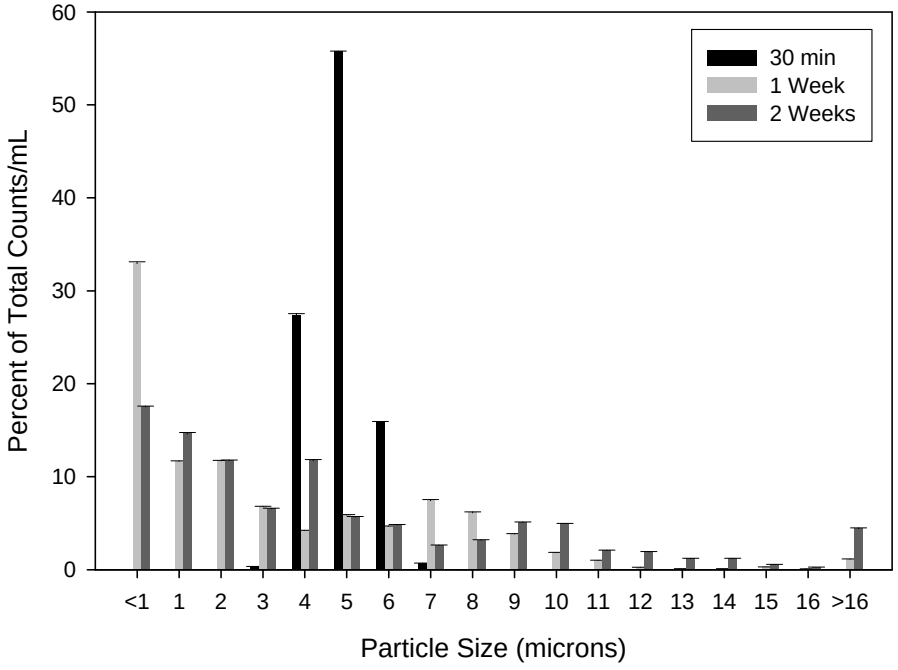


**Figure 4.16** Particle size distribution for 0.5 mg/L $Fe_2O_3$ solutions permanently maintained in a rotary tumbler.

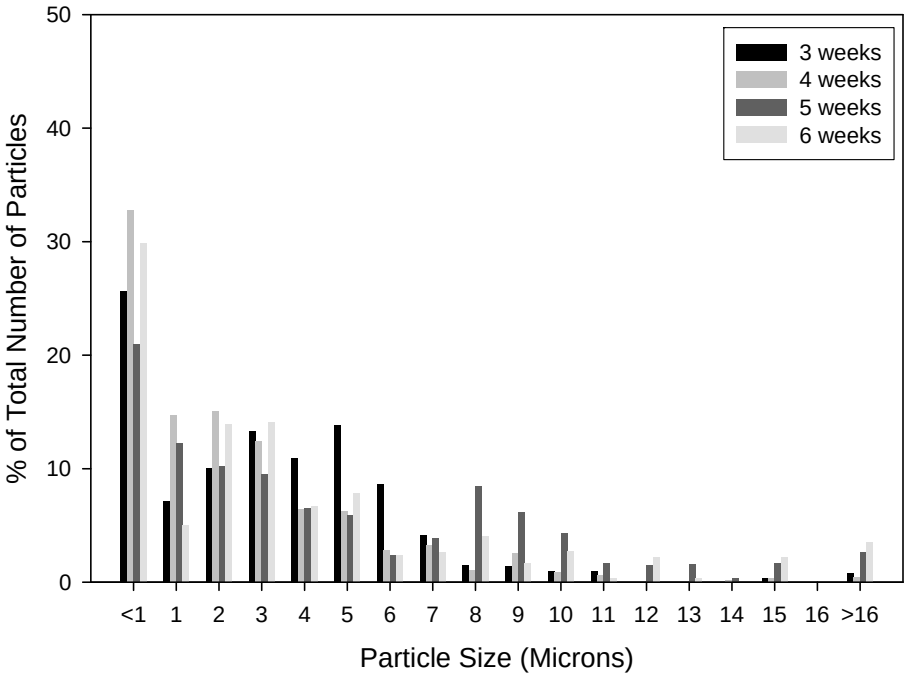


**Figure 4.17** Particle size distribution for 0.5 mg/L $Fe_2O_3$ solutions permanently maintained in a rotary tumbler (Represents a continuation of data in Figure 4.16).

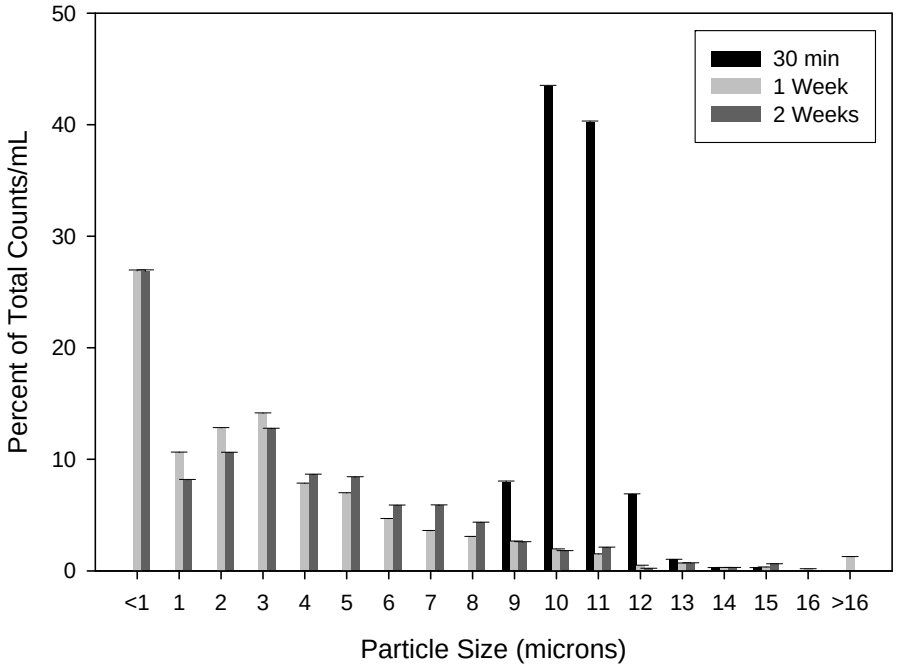


**Figure 4.18** Particle size distribution for 1.0 mg/L $Fe_2O_3$ solutions permanently maintained in a rotary tumbler.

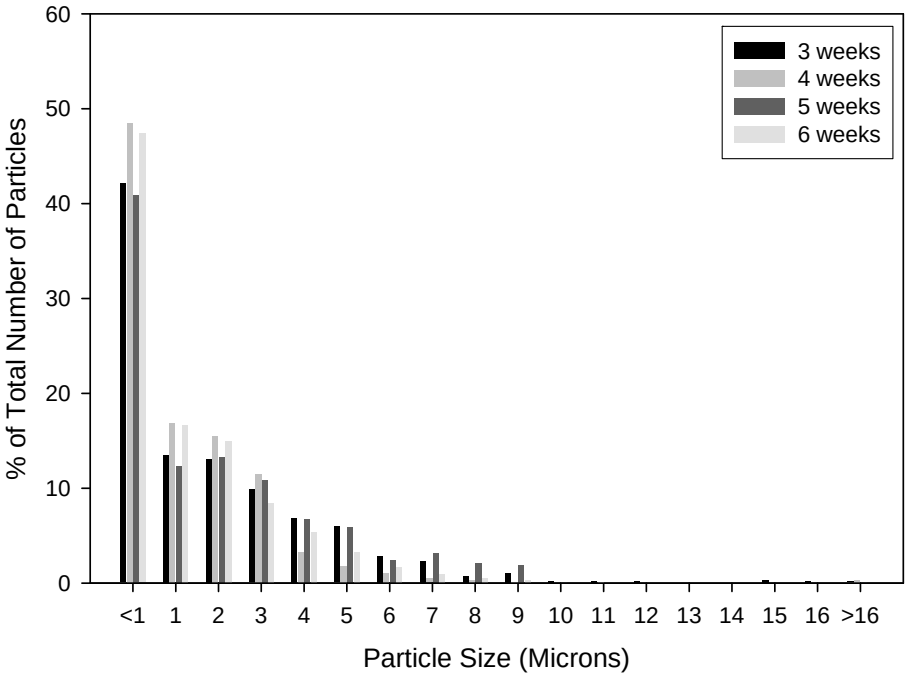


**Figure 4.19** Particle size distribution for 1.0 mg/L $Fe_2O_3$ solutions permanently maintained in a rotary tumbler (Represents a continuation of data in Figure 4.18).

## 5.0 Adsorption Isotherm Experimental Results

After the size distribution of $TiO_2$, $Fe_2O_3$, and $SiO_2$ nanoparticles was adequately evaluated, adsorption isotherms were conducted. This part of the study consisted of three main objectives. The first was to determine how $TiO_2$, $Fe_2O_3$, and $SiO_2$ nanoparticles impact the activated carbon adsorption of TCE. The second objective was to determine if the three nanomaterials evaluated in this study have the capacity to act as adsorption sites for TCE. The final objective was to evaluate how the presence of NOM affects the activated carbon adsorption of TCE in the presence of nanoparticles. The final objective was performed in order to more closely model conditions of drinking water sources. Figures 5.1 through 5.9 show the adsorption isotherm experimental results. A tabular form of the experimental data is provided in Appendix 1.

## 5.1 Single component Adsorption of TCE

Results for the adsorption isotherms for TCE onto PAC in the absence of any nanomaterials or humic acid are displayed in Figure 5.1. Two pH levels and six initial TCE concentrations ranging from 273 to 948 µg/L were used in these experiments. Figure 5.1 shows that on log-log coordinates, one linear correlation is attained over this concentration range. Furthermore, all isotherms conducted as part of this study displayed a linear $C_e$ to $Q_e$ relationship when plotted on log-log coordinates. Therefore, all isotherm results showed an independence of $C_o$. Isotherm experiments involving TCE alone were conducted in order to provide a baseline for comparing how the various nanoparticles would impact TCE adsorption. Figure 5.1 shows a significantly higher degree of TCE adsorption at an acidic pH. Solution pH is known to be a critical factor influencing

adsorption capacity of VOCs; and in general, VOCs are more readily adsorbed at lower pH's.

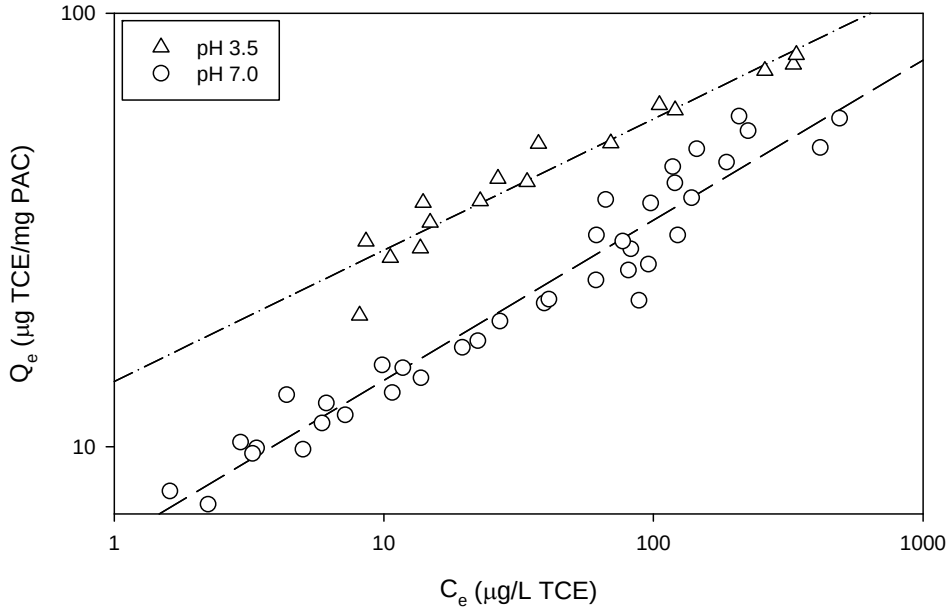


**Figure 5.1** Adsorption isotherm of TCE in nanopure water.

Figure 5.2 shows the isotherm plot for the experiment containing 20 nm $SiO_2$ at concentrations of 5.0 and 10 mg/L. Figure 5.2 shows no observable difference in TCE adsorption between the experiment conducted in nanopure water at a pH of 7.0 and the experiment conducted in the presence of $SiO_2$ nanoparticles. In addition, this experiment yielded similar Freundlich Parameters as the isotherm conducted in nanopure water (as shown in Table 5.1). This shows that silica nanoparticles had no impact on the adsorption of TCE onto activated carbon. This was to be expected because the PSD analysis previously performed did not show any aggregation of silica nanoparticles. This implies that the $SiO_2$ nanoparticles used in this experiment did not aggregate and act as adsorption sites for TCE.

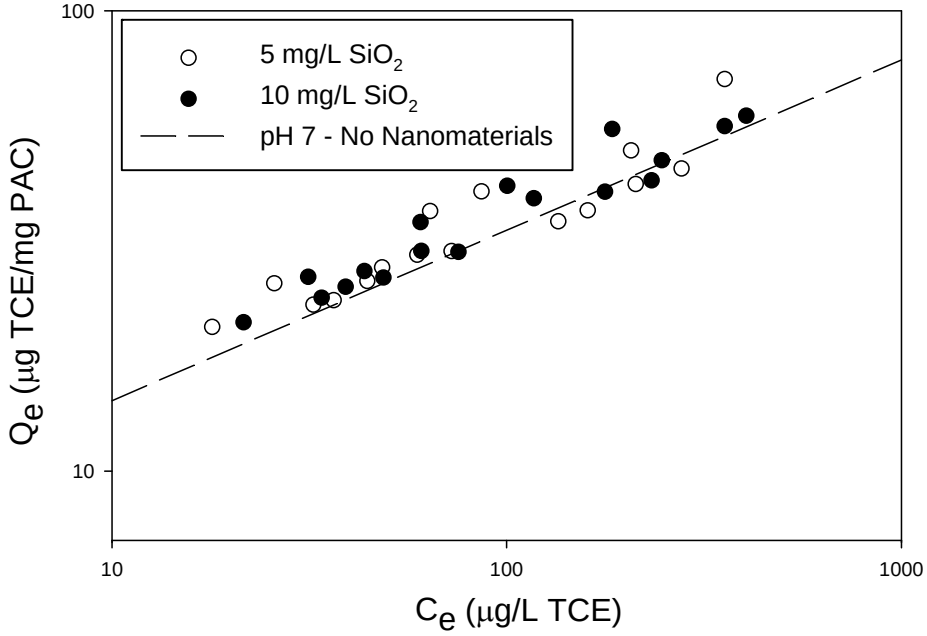


**Figure 5.2** Adsorption isotherms of TCE in the presence of $SiO_2$.

Figure 5.3 shows the isotherm plot for the experiment containing 30 nm $TiO_2$ particles at concentrations of 0.5 and 1.0 mg/L. A significantly higher degree of TCE adsorption is observed in the presence of $TiO_2$ compared to the baseline isotherm conducted in nanopure water. However, no difference in TCE adsorption was observed between the two $TiO_2$ concentration levels. TCE concentrations were analyzed for control bottles that contained 0.5 and 1.0 mg/L $TiO_2$, and no PAC. It was determined that at all three TCE concentration levels, the presence of $TiO_2$ nanoparticles alone removed 48% to 60% of TCE from the aqueous phase, regardless of $TiO_2$ concentration. Therefore, isotherm data showed that $TiO_2$ nanoparticles acted as adsorption sites for TCE. In fact, at a $C_e$ value of 100 µg/L, the presence of $TiO_2$ caused a 180% increase in $Q_e$ when compared to the baseline isotherm conducted with no nanomaterials. Therefore,

the change in TCE removal from the aqueous phase is very significant in the presence of $TiO_2$.

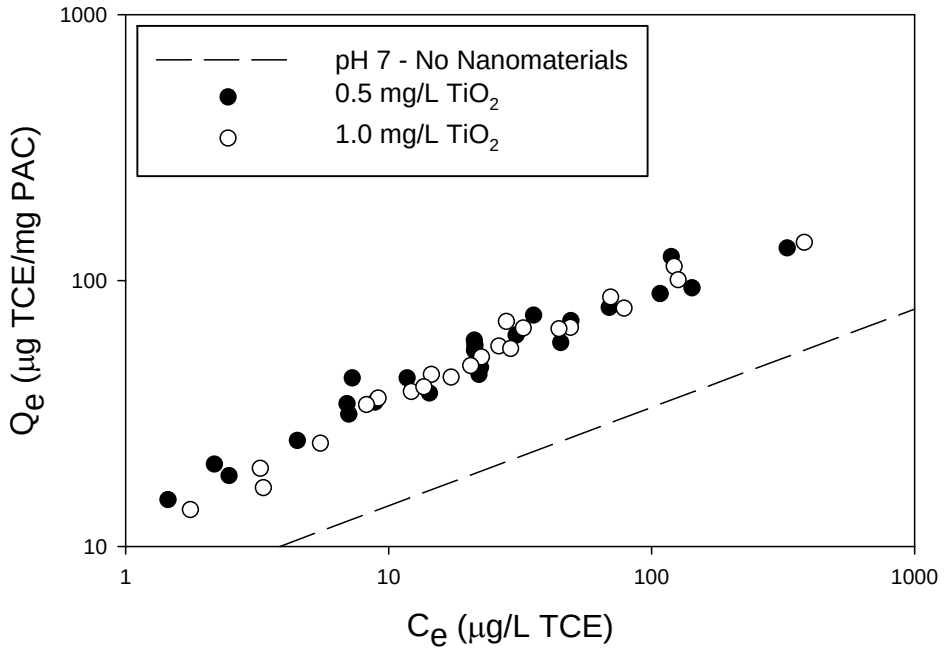


**Figure 5.3** Adsorption isotherms of TCE in the presence of $TiO_2$.

Figure 5.4 displays the isotherm conducted in the presence of 0.5 and 1.0 mg/L $Fe_2O_3$ nanoparticles at a pH of 3.5. The data showed an observable increase in the degree of TCE adsorption in the presence of $Fe_2O_3$ nanoparticles compared to the baseline isotherm conducted at a pH of 3.5 in the absence of nanomaterials. Similar to the $TiO_2$ isotherm, there was no observable difference in TCE adsorption between the two $Fe_2O_3$ concentration levels. Isotherm data also showed that $Fe_2O_3$ nanoparticles acted as adsorption sites for TCE. TCE concentrations were analyzed for control bottles that contained 0.5 and 1.0 mg/L $Fe_2O_3$, and no PAC. It was determined that at all three TCE concentration levels, the presence of $Fe_2O_3$ nanoparticles alone removed 42% to 53% of

TCE from the aqueous phase, regardless of $Fe_2O_3$ concentration. At a $C_e$ value of 100 μg/L, the presence of $Fe_2O_3$ caused a 47% increase in $Q_e$ when compared to the baseline isotherm conducted with no nanomaterials. Therefore, the change in TCE removal from the aqueous phase is very significant in the presence of $Fe_2O_3$ at higher $C_e$ values. However, $TiO_2$ increased the extent of TCE adsorption to a much greater extent than $Fe_2O_3$.

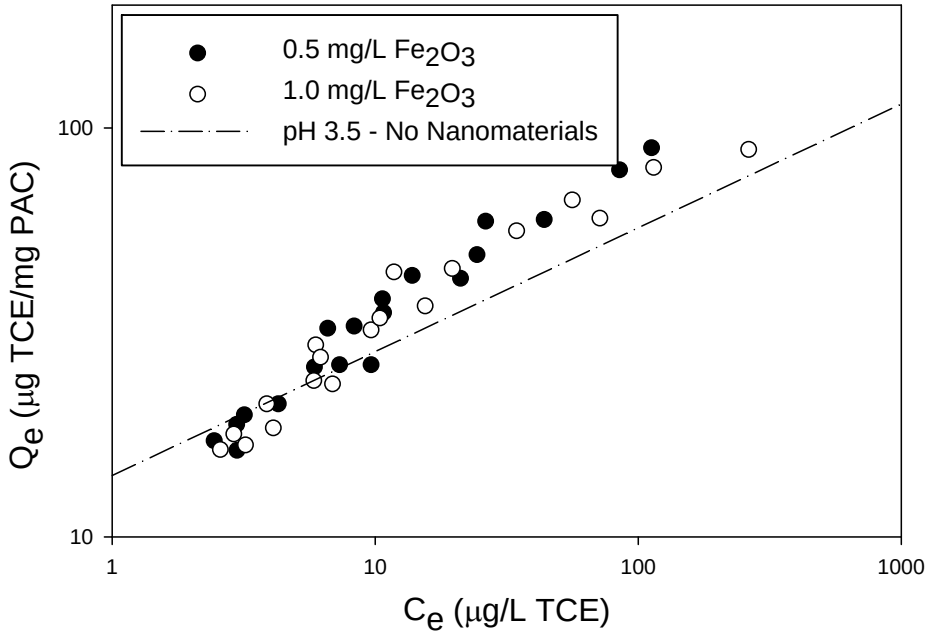


**Figure 5.4** Adsorption isotherms of TCE in the presence of $Fe_2O_3$.

In order to confirm that TCE was indeed being adsorbed by the $Fe_2O_3$ and titania, it was necessary to rule out the possibility of TCE degradation. Therefore, all chromatograms from analyzed TCE samples were examined for possible degradation products (such as dichloroethylene). Trace amounts of these compounds were found, but at levels <1% of the level of TCE. Therefore, TCE degradation played an insignificant

role in effecting isotherm data. In conclusion, the data shows that $TiO_2$ and $Fe_2O_3$ nanoparticles were acting as adsorption sites for TCE, which results in a higher degree of TCE removal from the aqueous phase. In turn, this causes the $C_e$ vs. $Q_e$ data to shift upward (as shown in Figures 5.3 and 5.4). Also, Table 5.1 shows that the change in Freundlich parameters between the two nanoparticle concentrations used for each isotherm was insignificant. Therefore, the concentration of $SiO_2$, $TiO_2$, and $Fe_2O_3$ had no bearing on the isotherm results. It is likely that the two nanoparticle concentration levels used were too comparable to result in any difference in adsorption.

**Table 5.1** Freundlich adsorption isotherm parameters for TCE adsorption on powdered activated carbon in the absence of Humic Acid

| Isotherm Parameters | 1/n | K | $R^2$ |
|---|---|---|---|
| pH 7.0 ± 0.2; No Nanomaterials | 0.37 | 6.07 | 0.94 |
| pH 3.5 ± 0.2; No Nanomaterials | 0.30 | 14.1 | 0.93 |
| 5 mg/L $SiO_2$ | 0.29 | 9.30 | 0.87 |
| 10 mg/L $SiO_2$ | 0.34 | 7.45 | 0.92 |
| 0.5 mg/L $TiO_2$ | 0.40 | 14.76 | 0.95 |
| 1.0 mg/L $TiO_2$ | 0.45 | 12.05 | 0.97 |
| 0.5 mg/L $Fe_2O_3$ | 0.44 | 11.76 | 0.96 |
| 1.0 mg/L $Fe_2O_3$ | 0.39 | 12.53 | 0.94 |

## 5.2 Impact of NOM on TCE Adsorption

The above isotherms were repeated in the presence of humic acid at a concentration of 5 mg/L in order to examine the adsorptive capacity of three nanomaterials in a system containing NOM. Figure 5.5 shows that presence of humic acid had impacted the adsorption of TCE at neutral and acidic pH. Humic acid had a more significant impact on TCE adsorption at pH 7 than at pH 3.5. Figure 5.5 shows that

the presence of humic acid decreased the adsorptive capacity of TCE. This result is to be expected because the presence of NOM often reduces the adsorption of organic micropollutants in multi-component systems. The exact mechanism that caused the decrease in TCE adsorption (i.e. pore blockage, direct site competition) was beyond the scope of this study and thus was not examined.

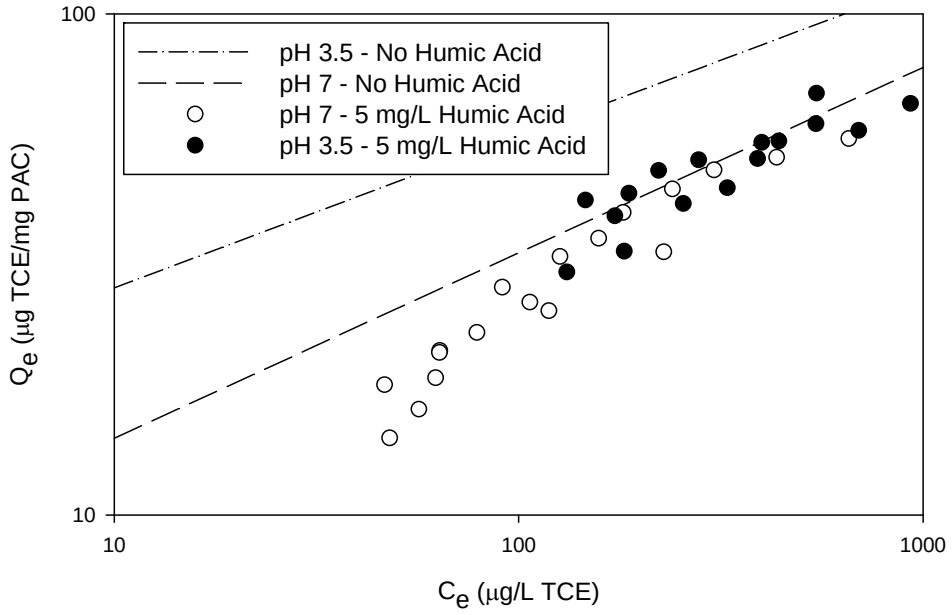


**Figure 5.5** Adsorption isotherms of TCE in nanopure water containing 5 mg/L humic acid.

Figure 5.6 shows the isotherm plot for the experiment conducted in the presence of 20 nm silica particles and 5 mg/L humic acid. The plot shows that the extent of TCE adsorption increased in the presence of silica, but no difference was observed between the 5 and 10 mg/L levels. Previous isotherm experiments performed with no humic acid showed that silica had no impact on TCE adsorption. It is likely that competition for PAC adsorption sites between TCE and humic acid impacted the fate of TCE in this system. TCE analysis of isotherm control bottles (containing no PAC) revealed that the

presence of silica removed 11% to 38% of TCE from the aqueous phase. Therefore, in a system with humic acid, it is seen in this study that silica particles were capable of adsorbing some TCE. At a $C_e$ value of 100 µg/L, the presence of $SiO_2$ caused an average of 64% increase in $Q_e$ for both $SiO_2$ concentrations when compared to the baseline isotherm conducted with no nanomaterials. Therefore, there is a significant increase in TCE adsorption in the presence of $SiO_2$.

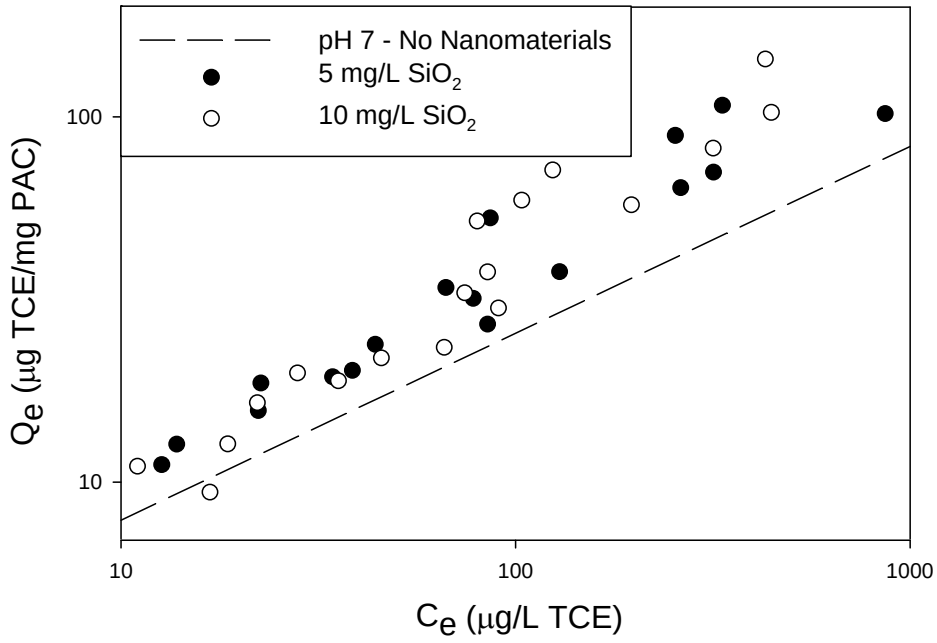


**Figure 5.6** Adsorption isotherms for TCE in the presence of 5 mg/L humic acid and $SiO_2$.

Isotherm experiments conducted with 0.5 and 1.0 mg/L $TiO_2$ at 5 mg/L humic acid are shown in Figure 5.7. The data shows that the presence of $TiO_2$, regardless of concentration, significantly decreased the remaining TCE in the aqueous phase; thus increasing the extent of adsorption. The impact that $TiO_2$ nanoparticles had on isotherms

conducted with and without humic acid was similar. More specifically, the data for $TiO_2$ isotherms plots the same distance above the baseline experiments regardless of humic acid. Analysis of control bottles (containing no PAC) showed that the presence of $TiO_2$ removed 36% to 54% of TCE from the aqueous phase, thus adsorbing the TCE. The data shows that humic acid impacted the extent of TCE adsorption onto the PAC, but had little impact on the adsorptive capability of $TiO_2$ for TCE. At a $C_e$ value of 100 µg/L, the presence of $TiO_2$ caused an average of 200% increase in $Q_e$ for both $TiO_2$ concentrations when compared to the baseline isotherm conducted with no nanomaterials. Therefore, there is a significant increase in TCE adsorption in the presence of $TiO_2$. This increase in $Q_e$ is very close to the increase observed for the $TiO_2$ isotherm conducted in the absence of humic acid.

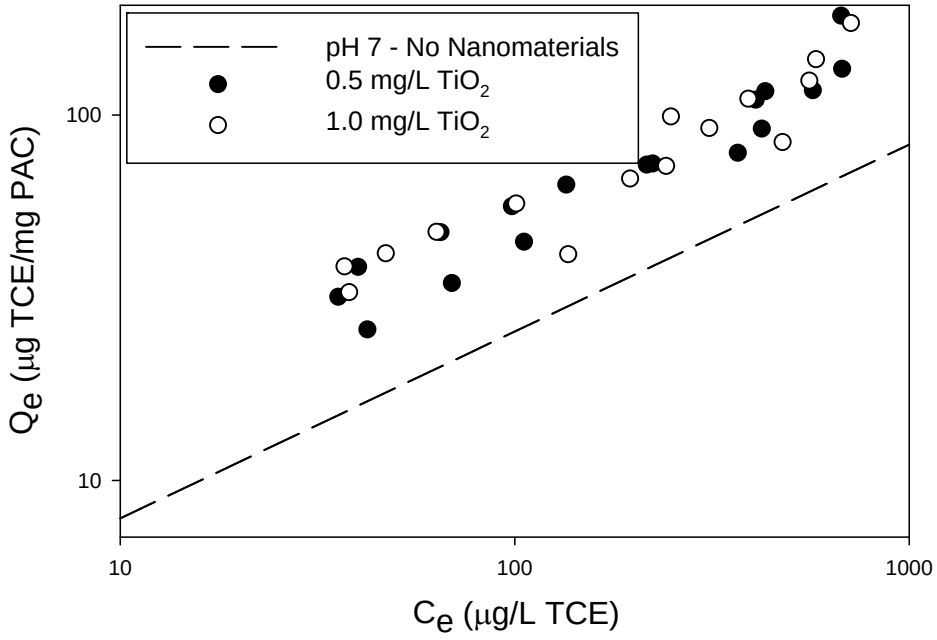


**Figure 5.7** Adsorption isotherms for TCE in the presence of 5 mg/L humic acid and $TiO_2$.

The impact of $Fe_2O_3$ nanoparticles on TCE adsorption, shown in Figure 5.8 was less dramatic than that of $TiO_2$ but was still significant. At both $Fe_2O_3$ concentrations, TCE adsorption increased, and both data sets plotted the same distance above the baseline. Therefore, the extent of TCE adsorption did not increase with increasing $Fe_2O_3$ concentration, which is consistent with previous experiments. Analysis of control bottles (containing no PAC) revealed that the presence of $Fe_2O_3$ nanoparticles, regardless of concentration, removed between 23% and 60% of TCE from the aqueous phase. At a $C_e$ value of 100 µg/L, the presence of $Fe_2O_3$ caused an average of 130% increase in $Q_e$ for both $Fe_2O_3$ concentrations when compared to the baseline isotherm conducted with no nanomaterials.

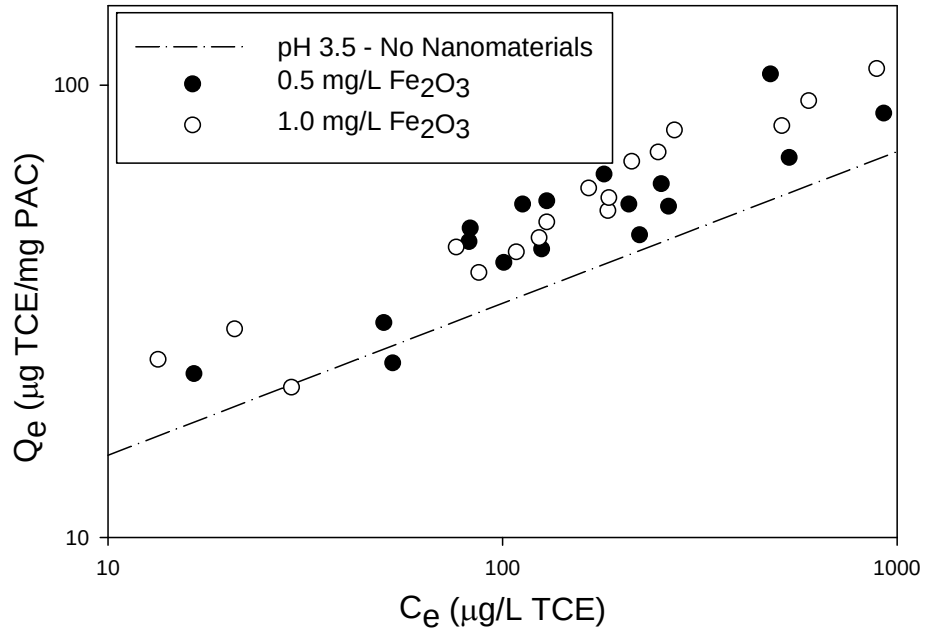


**Figure 5.8** Adsorption isotherms for TCE in the presence of 5 mg/L humic acid and $Fe_2O_3$.

Equilibrium humic acid concentrations were analyzed for each of the above isotherms and removal was found to be very similar for each (See Figure 5.9). As to be expected, increasing the mass of PAC in each bottle resulted in greater humic acid adsorption, and the extent of humic acid adsorption onto PAC was not dependent upon the type or concentration of nanoparticles present.

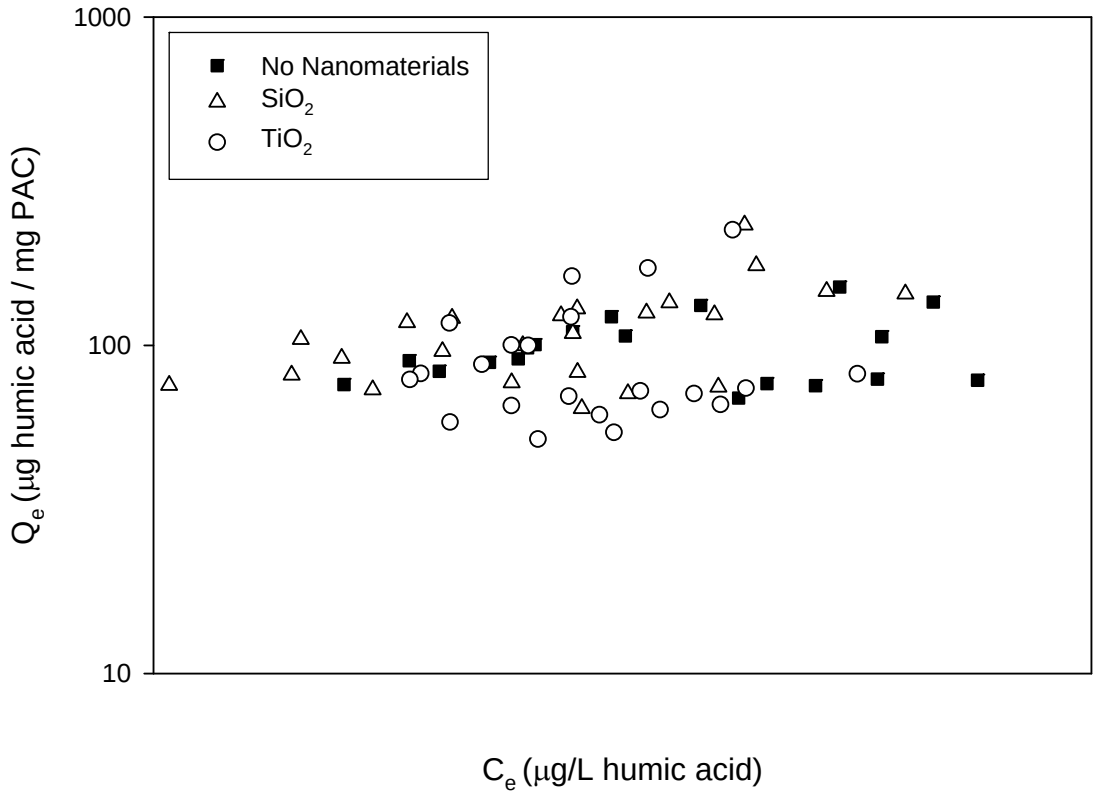


**Figure 5.9** Adsorption isotherms for humic acid in the presence of TCE and in the presence and absence of nanomaterials.

The presence of humic acid in the system generally increased the slope of the adsorption isotherm of TCE due to the increase in the value for *1/n*, as evidenced in Table 5.2. *K* values for isotherms conducted with humic acid were lower than the *K* values for isotherms without humic acid. The presence of humic acid was shown to decrease the

extent of TCE adsorption; and in turn, the Y-intercept of the humic acid isotherm plots was lower. According to the Freundlich model, this would result in a smaller *K* value. Table 5.2 shows that the change in Freundlich parameters between the two nanoparticle concentrations used for each isotherm was insignificant. Therefore, the concentration of $SiO_2$, $TiO_2$, and $Fe_2O_3$ had no bearing on the isotherm results. It is likely that the two nanoparticle concentration levels used were too comparable to result in any difference in adsorption.

**Table 5.2** Freundlich adsorption isotherm parameters for TCE adsorption on powdered activated carbon in the presence of Humic Acid

| Isotherm Parameters | 1/n | K | $R^2$ |
|---|---|---|---|
| pH 7.0 ± 0.2; No Nanomaterials | 0.51 | 2.42 | 0.93 |
| pH 3.5 ± 0.2; No Nanomaterials | 0.34 | 7.01 | 0.81 |
| 5 mg/L $SiO_2$ | 0.58 | 2.74 | 0.93 |
| 10 mg/L $SiO_2$ | 0.70 | 1.73 | 0.93 |
| 0.5 mg/L $TiO_2$ | 0.52 | 4.69 | 0.91 |
| 1.0 mg/L $TiO_2$ | 0.47 | 6.15 | 0.88 |
| 0.5 mg/L $Fe_2O_3$ | 0.37 | 7.85 | 0.81 |
| 1.0 mg/L $Fe_2O_3$ | 0.38 | 7.97 | 0.95 |

## 6.0 GAC Column Experimental Results

Isotherm experiments in the absence and presence of nanomaterials were conducted prior to the GAC column experiments in order to determine whether or not the nanoparticles impacted TCE adsorption. Once it was determined that the $TiO_2$, $Fe_2O_3$, and $SiO_2$ nanoparticles had the capacity to act as adsorption sites for TCE, it was necessary to design a GAC adsorber bed in order to adequately model drinking water treatment systems, which often use activated carbon as part of the treatment process. Due to the lengthy runtime for each GAC column experiment (approximately one month), only two experiments were completed. The first experiment was conducted in nanopure water at a pH 7.0 ± 0.2, and the second experiment was conducted at the same pH and in the presence of 5.0 mg/L $SiO_2$.

In order to design a GAC column experiment that would yield the breakthrough behavior targeted in these experiments, Environmental Technologies Design Option Tool (ETDOT) modeling software developed by Michigan Tech was used. More specifically, the Adsorption Design software program (AdDesignS) was used in the design of these experiments. ETDOT is a compilation of self-contained simulation software for use in assessing and implementing effective treatment strategies for gaseous, aqueous, organic, and solid waste by-product streams. AdDesignS is a ETDOT software that is specifically used in the design of fixed-bed adsorption processes (Mertz et. al, 1999). There are three models within this software that can be used; however, the pore and surface diffusion model (PSDM) was used for the column design according to the following assumptions and mechanisms. First, a constant flowrate and plug flow conditions are assumed. Also,

it is assumed that local adsorption equilibrium exists between the solute adsorbed onto the adsorbent particle and the intra-aggregate stagnant fluid. Finally, mass flux is described by surface and pore diffusion, and equilibrium is represented by the Freundlich isotherm equation (Mertz et. al, 1999).

Each design parameter for the GAC column was carefully selected. The bed length and flowrate were selected so that the EBCT was long enough so the TCE would not immediately breakthrough and be present in the effluent. The bed length and flowrate were also selected so that the mass transfer zone (MTZ) would be significantly shorter than the bed length. Filtrasorb 400 (F-400) from Calgon, Inc. was selected to be the adsorbent used in the column experiments because F-400 is very commonly used in drinking water treatment systems all over the U.S. The activated carbon used was sieved to the appropriate particle size range so that the ratio of the column diameter ($D_c$) to the particle diameter ($D_p$) was approximately 27. This was done to make sure that $D_c/D_p$ was greater than 25, a ratio where wall effects are generally negligible. The TCE concentration used in both experiments was 2.2 mg/L. This concentration was used because it was close to the highest TCE concentrations used in the isotherm experiments, and also low enough to realistically model the organic concentrations found in the influent of a typical treatment system. This influent concentration was also used to give the experiments a reasonable runtime (one month). If a significantly lower TCE concentration were used, complete breakthrough of the column would have taken several months.

Both experiments were conducted under identical conditions, with the exception of the second experiment being conducted in the presence of 5 mg/L 20 nm $SiO_2$. The

following parameters were entered into the AdDesignS model and used in each breakthrough experiment.

- Filtrasorb 400 GAC
- Freundlich Parameters: 1/n= 0.4354  K= 44.9 (mg/g)*(L/mg)^(1/n)
- Apparent Density = 0.40 g/$cm^3$
- Particle Diameter: 0.841 to 1.19 mm
- pH 7.0 ± 0.2
- No Humic Acid
- Flowrate: 15 mL/min
- $C_o$:  2.2 mg/L TCE
- Pore Diffusion Coefficient:  8.99 x $10^{-6}$ $cm^2$/s
- Film Diffusion Coefficient: 0.0114 cm/s
- Surface Diffusion Coefficient: 3.00 x $10^{-12}$ $cm^2$/s
- Mass of GAC:  15.9 grams
- Bed Length: 7.0 cm
- EBCT: 2.67 min.

Experimental and AdDesignS model results can be found in Figure 6.1.  Different breakthrough behavior was observed between the two experiments conducted.  The experiment conducted in the absence of nanomaterials breaks through significantly quicker than the experiment conducted in the presence of $SiO_2$.  One possible explanation for this is that $SiO_2$ particles in the influent were being trapped within the adsorber bed, where they were adsorbing some TCE.  This could account for the delayed breakthrough

observed in the $SiO_2$ experiment. Figure 5.2 in Chapter 5 shows that $SiO_2$ nanoparticles had no significant impact on TCE adsorption for the isotherm experiments performed with no humic acid. Therefore, one would expect to see no significant impact of $SiO_2$ on the breakthrough experiments. However, the isotherm experiments were performed with a peat-based PAC and the column experiments were performed with a bituminous coal based GAC, which possesses different physical and chemical properties. Figure 5.6 in Chapter 5.2 shows that $SiO_2$ nanoparticles had an impact on TCE adsorption in the isotherm experiments conducted at 5 mg/L humic acid. Therefore, it is postulated that $SiO_2$ may have the capacity to impact TCE adsorption under dynamic conditions. Further experiments need to be conducted in order to understand this situation. Analyses need to be conducted on the preloaded carbon in order to evaluate the attachment of $SiO_2$ on the carbon.

The ETDOT modeling prediction shown in Figure 6.1 is based upon ideal adsorption behavior. Therefore, the model prediction data will yield the classic carbon curve seen in Figure 6.1. Ideally, the model prediction should be very close to the data for the experiment conducted in nanopure water; however, the curve actually fell in between the two experiments performed in the lab.

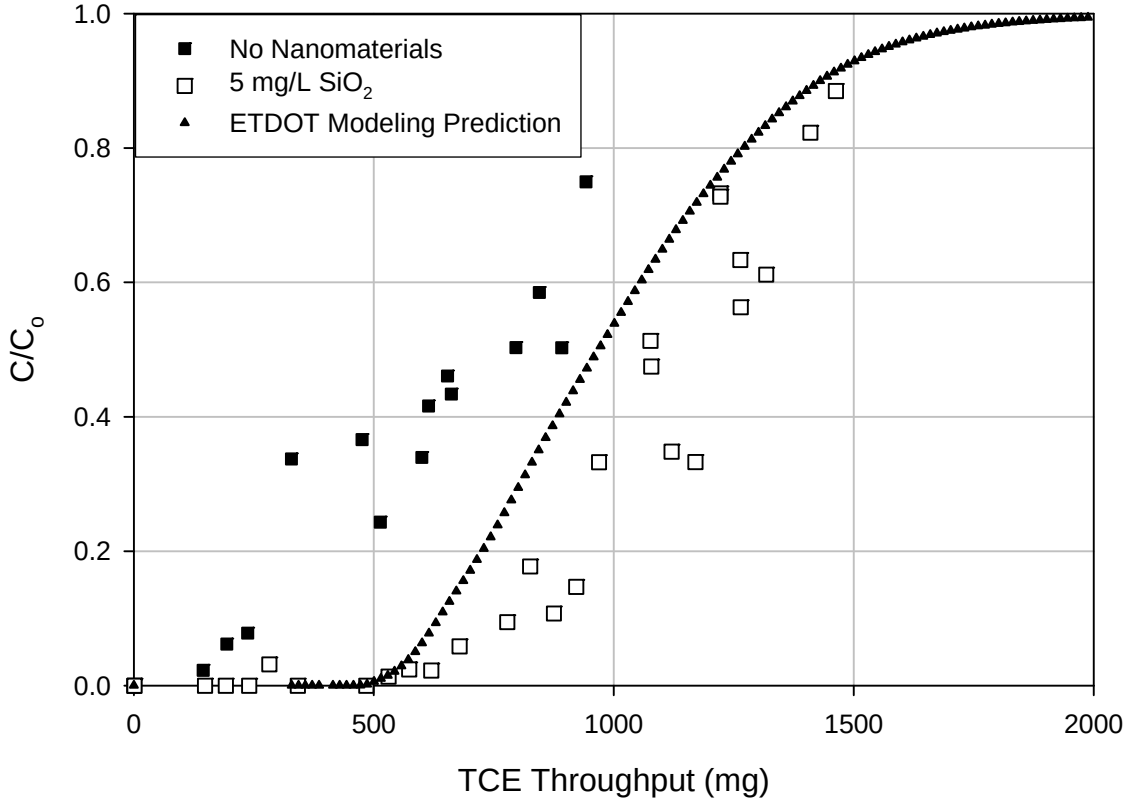


**Figure 6.1** Breakthrough plot for TCE in nanopure water and water containing 5 mg/L $SiO_2$ versus ETDOT modeling prediction.

Figure 6.2 shows influent pH data for both breakthrough experiments. The data shows that influent pH for both experiments were very similar and very close to 7.0. Figure 6.3 shows influent TCE concentration data ($C_o$) for both breakthrough experiments. This plot shows that $C_o$ values were nearly identical for both experiments. For the experiment performed with no nanomaterials: $C_o$ = 2.2 mg/L, standard deviation = 0.68 mg/L. For the experiment performed with 5 mg/L $SiO_2$: $C_o$ = 2.21 mg/L, standard deviation = 0.51 mg/L. As shown in the plot, $C_o$ data fluctuated between 1 and 3 mg/L. This variation can be easily explained. Although both tanks that held the influent solution were sealed with vacuum grease and kept under a nitrogen gas headspace, some

TCE was lost from the aqueous phase due to volatilization that would occur inside each tank as the level of water decreased and the amount of headspace increased.

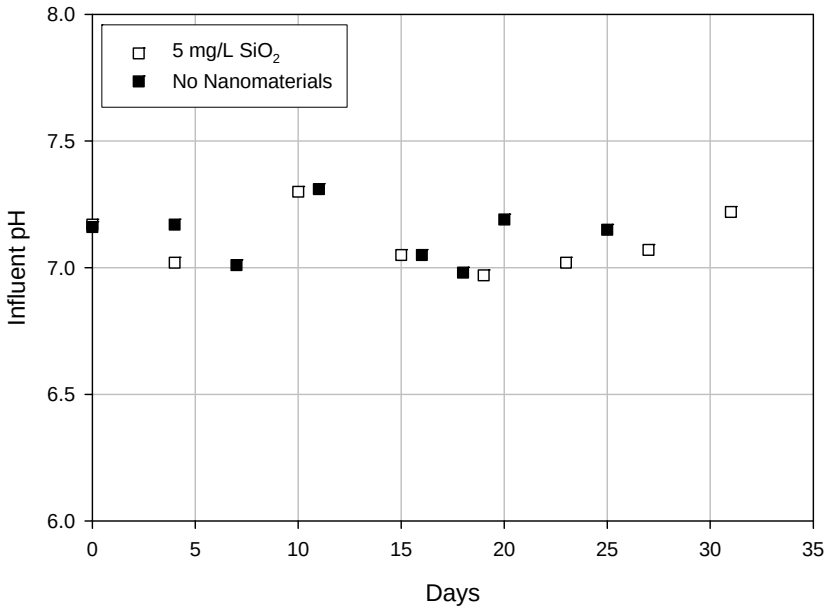


**Figure 6.2** Influent pH data for the breakthrough experiments shown in Figure 6.1.

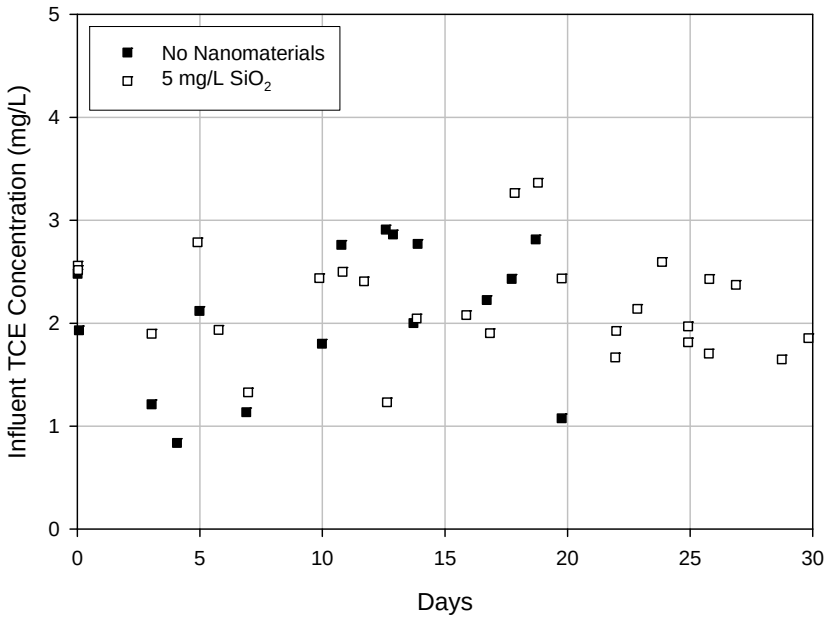


**Figure 6.3** Influent TCE concentration data for the breakthrough experiments shown in Figure 6.1.

Figure 6.4 shows the flowrate data for both breakthrough experiments. All data for the flowrate measurements was between 13 and 18 mL/min. Since a peristaltic pump was used to control flow through the column, some slight day to day variations in the flowrate are to be expected. For the experiment performed with no nanomaterials: flowrate = 15.05 mL/min, standard deviation = 1.04 mL/min. For the experiment performed with 5 mg/L $SiO_2$: flowrate = 15.43 mL/min, standard deviation = 0.82 mL/min. Therefore flowrate measurements were nearly identical for both breakthrough experiments.

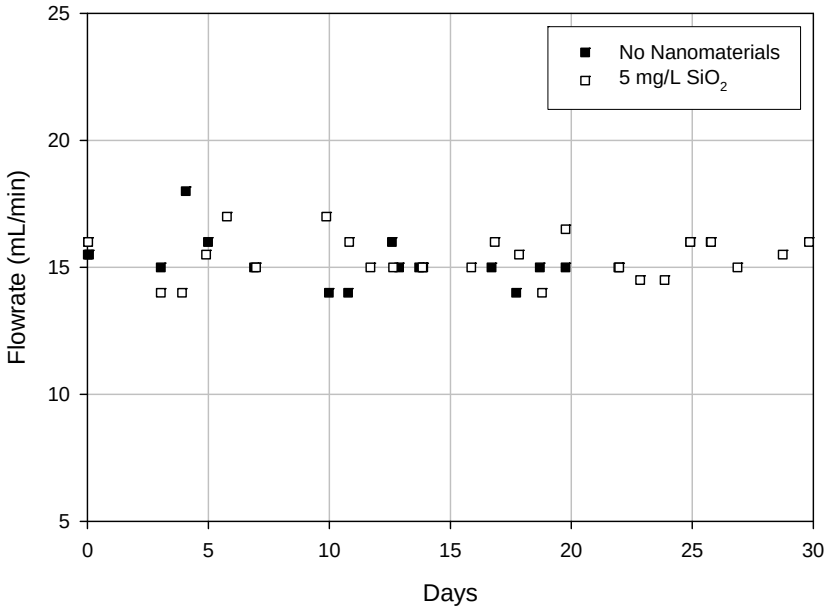


**Figure 6.4** Flowrate data for the breakthrough experiments shown in Figure 6.1.

## 7.0 Conclusions and Recommendations

This study evaluated the impact of three commercially available nanomaterials ($SiO_2$, $TiO_2$, and $Fe_2O_3$) on the adsorption of TCE by activated carbon. First, the size distribution in water of the three aforementioned nanoparticles was measured in order to determine the dominant size range of nanoparticle aggregates. This task was performed because larger nanoparticle aggregates tend to have a higher adsorptive capacity for various compounds. PSD was also measured with time in order to determine if these nanoparticle aggregates increase in diameter under continuous tumbling conditions. Next, adsorption isotherm experiments were conducted. Evaluations were conducted to determine if the three nanomaterials used in this study have the capability to act as adsorption sites for TCE, thereby impacting the activated carbon adsorption of this pollutant in the presence and absence of co-adsorbing NOM. Finally, a GAC column was designed and two breakthrough experiments were conducted for TCE. The first experiment was performed at neutral pH in the absence of nanomaterials. The second was performed under identical condition, with the exception that the influent solution contained 5 mg/L $SiO_2$. These experiments were performed in order to more closely model an actual treatment system, and to characterize the impact that nanomaterials have on the breakthrough of a GAC adsorber bed. The following conclusions about the three phases of this study (PSD, isotherms, breakthrough experiments) will be described separately below.

### 7.1 Particle Size Distribution (PSD)

During the duration of the PSD study, no particle counts greater than 1 μm were registered for both the 4 and 20 nm $SiO_2$ at both concentration levels under either stationary conditions or continuous tumbling. From this we can infer that no aggregation of $SiO_2$ nanoparticles greater than 1 μm occurred for the 4 and 20 nm $SiO_2$. One explanation for the apparent lack of aggregation is that both sizes of $SiO_2$ were obtained as colloidal dispersions in solution, whereas the $TiO_2$ and $Fe_2O_3$ were obtained as nanopowders.

Nanoparticle aggregates of both concentration levels of $TiO_2$ and $Fe_2O_3$ solutions that were left stationary on the bench-top were found to completely settle out of suspension within 3 to 4 weeks. This was concluded because no particle counts were registered by the particle counter, which only detects particles in suspension.

Both the 0.5 and 1.0 mg/L $TiO_2$ solutions exhibited a larger aggregate size than the $Fe_2O_3$ solutions. When continuously tumbled, both concentration levels of $TiO_2$ displayed a Gaussian distribution with mean particle diameters of approximately 8 μm and 11 μm for the 0.5 mg/L and 1.0 mg/L levels, respectively. A larger aggregate size was observed at a higher concentration. One explanation for this phenomenon is that at the higher concentration, each bottle contains twice the mass of $TiO_2$, which could allow a larger slightly larger aggregate to form. The size distributions for both concentrations of $TiO_2$ within the 1 to 16 μm range remained consistent throughout the duration of these experiments. From this data we can conclude that $TiO_2$ particles stabilize quickly when continuously tumbled and do not form larger aggregates with time.

Both the 0.5 and 1.0 mg/L $Fe_2O_3$ solutions exhibited a similar size distribution. When continuously tumbled, both concentration levels of $Fe_2O_3$ displayed a distribution that peaked at the 1 μm size and tailed off with increasing particle size. The size distributions for both concentrations of $Fe_2O_3$ within the 1 to 16 μm range remained consistent throughout the duration of these experiments. From this data we can conclude that like the $TiO_2$ particles, $Fe_2O_3$ particles stabilize quickly when continuously tumbled and do not form larger aggregates with time.

### 7.2 Adsorption Isotherm Experiments

Isotherm experiments were performed at pH 7.0 and pH 3.5 in the absence of nanomaterials in order to provide a baseline for comparing isotherm experiments involving $TiO_2$, $SiO_2$, and $Fe_2O_3$. At pH 3.5, the extent of TCE adsorption increased significantly compared to the experiment performed at neutral pH. These isotherms were repeated at a humic acid concentration of 5 mg/L. Humic acid was shown to have a more significant impact on TCE adsorption at pH 3.5 than at pH 7.0. The presence of humic acid decreased the adsorptive capacity of TCE as a result of competitive adsorption. This result is to be expected because the presence of NOM often reduces the adsorption of organic micropollutants in multi-component systems. The exact mechanism that caused the decrease in TCE adsorption (i.e. pore blockage, direct site competition) was beyond the scope of this study and thus was not examined.

Isotherms containing 5 and 10 mg/L $SiO_2$ in the presence and absence of humic acid were conducted. No impact on TCE adsorption was observed for isotherms that contained $SiO_2$ in humic acid-free water. However, $SiO_2$ particles had an impact on TCE

adsorption for isotherms containing humic acid and were shown to adsorb some TCE. Both concentrations of $SiO_2$ displayed the same impact on TCE adsorption; therefore, isotherms results were independent of $SiO_2$ concentration. The same phenomenon was observed for isotherms containing $TiO_2$ and $Fe_2O_3$. No difference in isotherm results was observed between the two nanoparticle concentration levels used, likely due to the narrow nanoparticle concentration range evaluated.

Isotherms containing $TiO_2$ were shown to increase the extent of TCE adsorption dramatically in the presence and absence of humic acid. For experiments containing $TiO_2$, TCE adsorption increased 180% and 200% in the absence and presence of humic acid, respectively. The observed increase in adsorption was caused by TCE being adsorbed by both the activated carbon as well as the $TiO_2$, which resulted in a greater extent of TCE removal from the aqueous phase. $TiO_2$ had the most significant impact on TCE adsorption of all nanomaterials evaluated.

Isotherms containing $Fe_2O_3$ were shown to increase the extent of TCE adsorption in the presence and absence of humic acid. For experiments containing $Fe_2O_3$, TCE adsorption increased 47% and 130% in the absence and presence of humic acid, respectively. Similar to the phenomena observed for $TiO_2$ isotherms, the observed increase in adsorption was caused by TCE being adsorbed by both the activated carbon as well as the $Fe_2O_3$, which resulted in a greater extent of TCE removal from the aqueous phase.

## 7.3 GAC Column Breakthrough Experiments

Two breakthrough experiments were conducted under identical conditions, with the exception of one experiment containing 5 mg/L $SiO_2$ in the influent water. Initial TCE breakthrough for the experiment containing $SiO_2$ occurred at approximately day 11, while breakthrough for the experiment performed in nanopure water occurred significantly quicker; at day 3. Therefore the presence of $SiO_2$ caused a delay in the initial breakthrough of TCE. After the initial breakthrough, the slope of the breakthrough curves for both experiments were nearly identical.

The AdDesignS$^{TM}$ modeling software used to test the predictability of the breakthrough experiment performed in nanopure water yielded an initial breakthrough at 11 days. After the initial breakthrough, the slope of the breakthrough curve of the modeling prediction was nearly identical to the slope of the breakthrough curve of both experiments.

## 7.4 Recommendations for Future Work

Below are research recommendations for future work on this project.

- Breakthough experiments must be conducted for $TiO_2$ and $Fe_2O_3$ in the presence and absence of humic acid in order to determine the impact these nanoparticles will have on the TCE breakthrough curve.
- Analyses need to be conducted (using X-ray diffraction) on the preloaded carbon used in column experiments in order to evaluate the attachment of nanomaterials on the carbon.

- Methods of nanoparticle dis-aggregation (i.e. sonication) should be evaluated.
- Isotherm experiments and breakthrough experiments should be conducted for multi-component systems using multiple organic pollutants.
- Isotherms and breakthrough experiments should be performed with different nanomaterials, such as alumina and zinc oxide.

## 8.0 References

Allen, T.J. (2008) Nanotech: teeny tiny particles, big risks. Mother Earth News, 24.

Apblett, A.W. (2006) Nanotechnology for Removal of Arsenic from Drinking Water. Paper presented at the 231st ACS National Meeting, Atlanta, GA, March 2006.

Binnie, C.; Kimber, M.; and Smethurst, G. (2002) Basic water treatment (3rd ed.) London: Thomas Telford Publishing. 291 pp.

Bottero, J.; Rose, J.; Wiesner, M. (2006) Nanotechnologies: Tools for sustainability in a new wave of water treatment processes. *Integrated Environmental Assessment and Management*, 2(4), 391-395.

Brady, R.D. (1998). Activated Carbon Processes. *Water Treatment Plant Design* (3rd ed.). (377-415). New York: McGraw-Hill.

Carey, M. A.; Fretwell, B. A.; Mosley N. G.; Smith J. W. N. (2002) Guidance on the use of permeable reactive barriers for remediating contaminated groundwater. National Groundwater and Contaminated Land Centre Report NC/01/51. Environmental Agency, UK. <http://66.102.1.104/scholar?num=20&hl=en&lr=&q=cache:6L6K5mJZ_XUJ:publications.environmentagency.gov.uk/pdf/SCHO0902BITMe.pdf+Remedial+Methods+for+Contaminated+Groundwater+author:Smith> 6 Aug. 2008.

Cheremisinoff, N. P. (2002). Handbook of water and wastewater treatment technologies (1st ed.).(372-445). Boston: Butterworth-Heinemann.

Clark, R.M. and Lykins Jr., B.W. (1989). Granular activated carbon: Design, operation, and cost (1st ed.). Chelsea, Michigan: Lewis Publishers. 342 pp.

Ebie, K.; Li, F.; Azuma, Y.; Yuasa, A.; Hagishita, T. (2001). "Pore distribution effect of activated carbon in adsorbing organic micropollutants from natural water." *Water Resources*, 35(1), 167-169.

Faur, C.; Metivier-Pignon, H.; Le Cloirec, P. (2005). "Multicomponent Adsorption of Pesticides onto Activated Carbon Fibers." *Adsorption*, 11, 479-490.

Faust, S.D. and Aly, O.M. (1987). Adsorption processes for water treatment (1st ed.). Boston: Butterworth Publishers. 509 pp.

Guzman, K.A.; Taylor, M.R.; Banfield, J.F. (2006) Environmental risks of nanotechnology: national nanotechnology intitiative funding, 2000-2004, *Environmental Science and Technology,* 40(5), 1401-1407.

Hannah, W. and Thompson, P.B. (2008) Nanotechnology, risk and the environment: a review. *Journal of Environmental Monitoring*, 10, 291-300.

Holman, M.W.; Kemsley, J.; Nordan, M.M.; Sullivan, T.; Mamikunian, V.; Nagy, C.; Lackner, D.I.; Munger, M.; Beigala, T.; Jabbawy, B.; Yoo, R.; Kusari, U.; Dobbins, M. *The Nanotech Report*$^{TM}$*: Investment overwiew and market research for nanotechnology* ($4^{th}$ ed.). Lux Research, New York, 2006. 623 pp.

Hristovski, K. et al. (2007) Simultaneous removal of perchlorate and arsenate by ion-exchange media modified with nanostructured iron (hydr)oxide. *Journal of Hazardous Materials***[In Press].**

Jia, G.: Wang, H.F.; Yan, L.; Wang, X.; Pei, R.J.; Yan, T.; Zhao, Y.L.; Guo, X.B. (2005) Cytotoxicity of carbon nanomaterials: Single-wall nanotube, multi-wall nanotube, and fullerene. *Environmental Science and Technology,* 39, 1378-1383.

Kilduff, J. and Karanfil, T. (2002) Trichloroethylene adsorption by activated carbon preloaded with humic substances: effects of solution chemistry. *Water Research* 36, 1685-1698.

Kilduff, J.; Karanfil, T.; and Weber, W. (1998) Competitive Effects of Nondisplaceable Organic Compounds on Trichloroethylene Uptake by Activated Carbon. I. Thermodynamic Predictions and Model Sensitivity Analyses. *Journal of Colloid and Interface Science*, 205, 271-279.

Kilduff, J. and Weber W. J. (1994) Factors affecting the impacts of dissolved organic matter preloading on the GAC adsorption of trichloroethylene. Proc. American Water Works Association Annual Conference. New York City, New York.

Liu, H.B. and Xiao, H.N. (2007) Adsorption of poly(ethylene oxide) with different molecular weights on the surface of silica nanoparticles and the suspension stability. *Materials Letters*, 62(6-7), 870-873

Matsui, Y.; Fukuda, Y.; Inoue, T.; Matsushita, T. (2003). "Effect of natural organic matter on powdered activated carbon adsorption of trace contaminants: characteristics and mechanism of competitive adsorption." *Water Research*, 37, 4413-4424.

Mertz, K.A., Gobin, D., Hand, D.W., Hokanson, D.R., and Crittenden, J.C. "Adsorption Design Software for Windows AdDesign$^{TM}$". Michigan Technological University. Houghton, MI, 1999.

Nakagawa, Y.; Wakuri, S.; Sakamoto, K.; Tanaka, N. (1997) The photogenotoxicity of titanium dioxide particles. *Mutagen Research – Genetic Toxicology Environmental Mutagen,* 394, 125-132.

Nanoscience and nanotechnologies: opportunities and uncertainties. (2004) (1st ed.). *The Royal Society and the Royal Academy of Engineering.* 116 pp.

Nanomaterials – a risk to health at work? First International Symposium on Occupational Health Implications of Nanomaterials, 12-14 Oct 2004, Health and Safety Laboratory. <http://www.hsl.gov.uk/capabilities/nanosymrep_final.pdf> 22 July 2008.

National Primary Drinking Water Regulations: Technical Factsheet on Trichloroethylene. U.S. Environmental Protection Agency. <www.epa.gov/OGWDW/dwh/t-voc/trichlor.html> 6 Aug. 2008.

Newcombe, G.; Morrison, J.; Hepplewhite, C.; Knappe, D.R.U. (2002) Simultaneous adsorption of MIB and NOM onto activated carbon: II. Competitive effects. *Carbon*, 40, 2147-2156.

Otake, Y.; Kalili, N.; Chang, T.H.; Furuya, E. (2004) Relationship between Freundlich-type equation constants and molecular orbital properties. *Separation and Purification Technology*, 39, 67-72.

Pacheco, S.; Tapia, J.; Medina, M.; Rodriguez, R. (2006) Cadmium ions adsorption in simulated wastewater using structured alumina-silica nanoparticles. *Journal of Non-Crystalline Solids*, 352(52-54) 5475-5481.

Quinlivan, P.; Li, L.; Knappe, D. (2005) Effects of activated carbon characteristics on the simultaneous adsorption of aqueous organic micropollutants and natural organic matter. *Water Research,* 39, 1663-1673.

Rahman, Q.; Lohani, M.; Dopp, E.; Pemsel, H.; Jonas, L.; Weiss, D.G.; Schiffman, D. (2002) Evidence that ultrafine titanium dioxide induces micronuclei and apoptosis in Syrian hamster embryo fibroblasts. *Environmental Health Perspect,* 110, 797-800.

Ram, N.M.; Christman, R.F.; and Cantor, K.P. (1990). Significance and treatment of volatile organic compounds in water supplies (1st ed.). Chelsea, Michigan: Lewis Publishers. 558 pp.

Senftle, F.E.; Thorpe, A.N.; Grant, J.R.; Barkatt, A. (2007) Superparamagnetic Nanoparticles in Tap Water. *Water Research*, 41, 3005-3011.

Shani, M; Finney, WC; Clark, RJ; Landing, W; Locke, BR. Degradation of Aqueous Phase Trichloroethylene Using Pulsed Corona Discharge. Hakone VIII International Symposium on High Pressure Low Temperature Plasma Chemistry. 21-25 July 2002. Puhajarve, Estonia.

Sharpe, M. (2006) Small wonders, big future: the development of environmental nanotechnology. *Journal of Environmental Monitoring*, 8, 235-239.

Stenzel, M.H. and Gupta, S.U., (1995) Air pollution control with granular activated carbon and air stripping. *Journal of Hazardous Waste Management* 35 (12), 1304–1309.

Wiesner, M.R. (2006) Responsible development of nanotechnologies for water and wastewater treatment. *Water Science & Technology*, 53(3) 45–51.

Zheng, F.; Li, S.; Qian, S.; Dang, N. (2007) Surface-modification of titania nanoparticles with salicyclic acid and 5-sulfosalicylic acid to remove p-nitrophenol by adsorption. *Journal of Environmental Science*, 27(1), 64-68.

# APPENDICES

## APPENDIX 1: $C_e$ (µg/L TCE) vs. $Q_e$ (µg TCE/mg PAC) Data for Adsorption Isotherm Experiments

### Nanopure Water – No Humic Acid

**pH 3.5**

| $C_e$ | $Q_e$ |
|---|---|
| 8.137103 | 20.07859 |
| 330.2022 | 76.22081 |
| 105.2922 | 61.44165 |
| 37.4955 | 50.03333 |
| 34.01482 | 40.83336 |
| 13.97699 | 36.5472 |
| 8.588043 | 29.75836 |
| 10.56808 | 27.27862 |
| 338.9267 | 80.16251 |
| 259.3235 | 73.65268 |
| 120.4687 | 59.78114 |
| 69.5324 | 50.1402 |
| 26.51605 | 41.52539 |
| 22.78761 | 36.8535 |
| 14.84543 | 32.89123 |
| 13.66643 | 28.68689 |

**pH 7.0**

| $C_e$ | $Q_e$ |
|---|---|
| 11.76187 | 15.2059 |
| 13.74356 | 14.41999 |
| 4.357472 | 13.18362 |
| 6.114339 | 12.60326 |
| 5.901046 | 11.33061 |
| 2.940824 | 10.241 |
| 3.372902 | 9.923914 |
| 3.260859 | 9.644375 |
| 1.608983 | 7.898092 |
| 2.229375 | 7.366141 |
| 97.75153 | 36.47521 |
| 95.7742 | 26.36102 |
| 39.35453 | 21.45736 |
| 19.56286 | 16.95033 |
| 7.193998 | 11.84232 |
| 123.0547 | 30.78254 |
| 61.46599 | 30.78348 |
| 82.44805 | 28.58946 |
| 80.81933 | 25.55373 |
| 88.41851 | 21.76719 |
| 26.93542 | 19.47775 |
| 22.32837 | 17.5621 |
| 9.858396 | 15.43566 |
| 10.75323 | 13.32994 |
| 5.012184 | 9.86016 |
| 138.5252 | 37.51571 |
| 76.9561 | 29.82081 |
| 61.19656 | 24.23977 |
| 40.96251 | 21.88598 |
| 415.9401 | 48.97995 |
| 224.4387 | 53.55436 |
| 144.7192 | 48.67327 |
| 117.9906 | 44.2639 |
| 66.56541 | 37.16358 |
| 490.4528 | 57.26539 |
| 207.803 | 57.87288 |
| 186.7573 | 45.34635 |
| 120.2 | 40.60666 |

## $SiO_2$ – No Humic Acid

**5.0 mg/L $SiO_2$**

| $C_e$ | $Q_e$ |
|---|---|
| 160.4173 | 36.81588 |
| 59.34287 | 29.50353 |
| 48.37506 | 27.69164 |
| 32.38278 | 22.97682 |
| 356.6965 | 71.03847 |
| 206.6894 | 49.67568 |
| 86.34769 | 40.49882 |
| 63.98517 | 36.68072 |
| 25.77708 | 25.5794 |
| 17.94632 | 20.56401 |
| 277.3264 | 45.39955 |
| 212.3059 | 42.02464 |
| 135.1575 | 34.85254 |
| 72.5231 | 30.03409 |
| 44.35935 | 25.85714 |
| 36.47684 | 23.49214 |

**10.0 mg/L $SiO_2$**

| $C_e$ | $Q_e$ |
|---|---|
| 117.1076 | 39.12099 |
| 60.79007 | 30.07876 |
| 31.43477 | 26.42468 |
| 21.53578 | 21.03884 |
| 404.4243 | 59.1411 |
| 185.196 | 55.34549 |
| 100.2958 | 41.62387 |
| 60.48831 | 34.73265 |
| 43.63417 | 27.1799 |
| 39.08197 | 25.12991 |
| 356.6461 | 56.15297 |
| 247.2022 | 47.33059 |
| 232.7984 | 42.77051 |
| 177.4644 | 40.40475 |
| 75.46297 | 29.93738 |
| 48.71645 | 26.31581 |

## $TiO_2$ – No Humic Acid

**0.5 mg/L $TiO_2$**

| $C_e$ | $Q_e$ |
|---|---|
| 107.7431 | 89.17051 |
| 49.28917 | 70.53125 |
| 21.20536 | 54.55584 |
| 7.266421 | 43.03392 |
| 21.16664 | 59.7209 |
| 6.953087 | 34.41856 |
| 4.496819 | 25.02918 |
| 2.175932 | 20.38231 |
| 2.470551 | 18.45996 |
| 1.447959 | 14.98726 |
| 118.8628 | 123.0974 |
| 35.5889 | 74.13234 |
| 30.54613 | 62.28639 |
| 21.28898 | 56.9477 |
| 11.76621 | 43.04143 |
| 8.877058 | 34.90119 |
| 7.053341 | 31.42187 |
| 327.7807 | 132.4638 |
| 142.5036 | 93.81658 |
| 69.02088 | 79.13564 |
| 45.11689 | 58.40103 |
| 22.33248 | 47.1516 |
| 22.03908 | 44.31998 |
| 14.28912 | 37.73401 |

**1.0 mg/L $TiO_2$**

| $C_e$ | $Q_e$ |
|---|---|
| 69.79095 | 86.56236 |
| 28.03865 | 70.10674 |
| 22.54227 | 51.57352 |
| 17.27502 | 43.30277 |
| 49.123 | 66.55038 |
| 14.53075 | 44.28026 |
| 5.497835 | 24.45561 |
| 3.251548 | 19.65808 |
| 3.339827 | 16.60935 |
| 1.764314 | 13.75817 |
| 121.7435 | 112.9616 |
| 32.51491 | 66.24154 |
| 26.24478 | 56.71826 |
| 12.19969 | 38.24567 |
| 9.123193 | 36.11151 |
| 8.233504 | 34.15181 |
| 30.2067 | 6.84335 |
| 380.66 | 139.1003 |
| 126.1834 | 100.5352 |
| 78.59834 | 78.60356 |
| 44.4157 | 65.86576 |
| 29.10094 | 55.46824 |
| 20.50953 | 47.82314 |
| 13.6048 | 39.78112 |

## $Fe_2O_3$ – No Humic Acid

**0.5 mg/L $Fe_2O_3$**

| $C_e$ | $Q_e$ |
|---|---|
| 84.8605 | 79.06195 |
| 21.09956 | 42.87849 |
| 5.87437 | 26.02797 |
| 3.180631 | 19.88669 |
| 2.98429 | 16.27836 |
| 112.4779 | 89.49222 |
| 26.28881 | 59.12257 |
| 24.39434 | 48.9809 |
| 13.8092 | 43.61813 |
| 10.76234 | 35.35735 |
| 6.599527 | 32.39367 |
| 9.646368 | 26.36609 |
| 43.90145 | 59.71311 |
| 10.64558 | 38.20329 |
| 8.317949 | 32.75449 |
| 7.316909 | 26.38111 |
| 4.280156 | 21.14107 |
| 2.973667 | 18.83743 |
| 2.441537 | 17.18513 |

**1.0 mg/L $Fe_2O_3$**

| $C_e$ | $Q_e$ |
|---|---|
| 71.49393 | 60.20652 |
| 9.64487 | 32.05214 |
| 6.877097 | 23.65867 |
| 4.101119 | 18.47552 |
| 3.215172 | 16.77804 |
| 262.8767 | 88.67276 |
| 114.5773 | 80.05342 |
| 56.12986 | 66.69373 |
| 34.50883 | 56.03823 |
| 11.78895 | 44.45725 |
| 15.49792 | 36.70354 |
| 5.943185 | 29.46744 |
| 19.62164 | 45.33362 |
| 10.41178 | 34.29999 |
| 6.198213 | 27.51497 |
| 5.849836 | 24.09115 |
| 3.870282 | 21.15708 |
| 2.900424 | 17.84839 |
| 2.576118 | 16.35288 |

## Nanopure Water Containing 5 mg/L Humic Acid

**pH 7.0**

| $C_e$ | $Q_e$ |
|---|---|
| 106.5854 | 26.59259 |
| 63.82259 | 21.286 |
| 46.61686 | 18.1979 |
| 56.69288 | 16.26157 |
| 47.99906 | 14.24898 |
| 228.5721 | 33.52284 |
| 118.7964 | 25.56839 |
| 78.86661 | 23.13309 |
| 63.73732 | 21.08806 |
| 62.34096 | 18.78804 |
| 655.6552 | 56.36644 |
| 434.6379 | 51.7454 |
| 304.1822 | 48.83771 |
| 240.1842 | 44.71795 |
| 181.4386 | 40.16771 |
| 157.8105 | 35.65973 |
| 126.637 | 32.80086 |
| 91.12174 | 28.48377 |

**pH 3.5**

| $C_e$ | $Q_e$ |
|---|---|
| 545.5099 | 69.46747 |
| 221.9723 | 48.70674 |
| 146.248 | 42.50348 |
| 182.5106 | 33.61225 |
| 131.5924 | 30.54126 |
| 1077.845 | 67.93547 |
| 543.5511 | 60.37861 |
| 399.4243 | 55.40985 |
| 278.7449 | 51.13188 |
| 187.3881 | 43.85369 |
| 173.0429 | 39.53056 |
| 931.3032 | 66.26143 |
| 693.5368 | 58.57863 |
| 440.3589 | 55.74293 |
| 389.9766 | 51.41877 |
| 328.2748 | 44.99141 |
| 255.5124 | 41.8298 |

## $SiO_2$ – 5 mg/L Humic Acid

**5.0 mg/L $SiO_2$**

| $C_e$ | $Q_e$ |
|---|---|
| 66.61264 | 34.11321 |
| 34.38118 | 19.42656 |
| 22.28939 | 15.69847 |
| 13.85246 | 12.71116 |
| 12.69471 | 11.16749 |
| 129.2608 | 37.68858 |
| 78.0765 | 31.83932 |
| 84.99844 | 27.06705 |
| 44.10474 | 23.84139 |
| 38.60025 | 20.22948 |
| 22.62974 | 18.66751 |
| 864.7429 | 102.1195 |
| 334.2886 | 107.6012 |
| 254.2844 | 88.96285 |
| 317.8225 | 70.56857 |
| 262.128 | 64.02531 |
| 86.25415 | 52.88885 |

**10.0 mg/L $SiO_2$**

| $C_e$ | $Q_e$ |
|---|---|
| 74.37914 | 32.97107 |
| 28.03034 | 19.89354 |
| 18.64745 | 12.72432 |
| 16.81539 | 9.392235 |
| 11.01436 | 11.06031 |
| 196.5817 | 57.44835 |
| 84.9262 | 37.63421 |
| 90.5109 | 29.98119 |
| 65.9837 | 23.38763 |
| 45.73187 | 21.87984 |
| 35.57661 | 18.9361 |
| 22.17502 | 16.50369 |
| 429.7278 | 143.9479 |
| 445.0992 | 102.8949 |
| 317.0238 | 82.13072 |
| 124.2073 | 71.5309 |
| 103.6952 | 59.19126 |
| 79.99654 | 51.87611 |

## $TiO_2$ – 5 mg/L Humic Acid

**0.5 mg/L $TiO_2$**

| $C_e$ | $Q_e$ |
|---|---|
| 165.8613 | 83.79893 |
| 105.6303 | 45.00455 |
| 69.31511 | 34.70724 |
| 42.33296 | 25.87168 |
| 672.3436 | 187.0232 |
| 676.2502 | 133.9565 |
| 569.8299 | 116.8736 |
| 408.1136 | 110.199 |
| 423.1624 | 91.82051 |
| 367.9777 | 78.78045 |
| 223.7011 | 73.67042 |
| 431.9563 | 116.2665 |
| 216.1148 | 73.12226 |
| 135.1349 | 64.42843 |
| 98.36547 | 56.28413 |
| 64.85604 | 47.78648 |
| 40.12185 | 38.4048 |
| 35.67085 | 31.78878 |

**1.0 mg/L $TiO_2$**

| $C_e$ | $Q_e$ |
|---|---|
| 241.9041 | 72.61617 |
| 136.6309 | 41.60161 |
| 711.417 | 178.6495 |
| 580.645 | 142.2447 |
| 558.0656 | 124.1819 |
| 391.1261 | 110.884 |
| 248.9012 | 99.04618 |
| 477.3475 | 84.29437 |
| 162.5015 | 78.38285 |
| 311.1704 | 92.10625 |
| 196.2704 | 67.05031 |
| 100.8561 | 57.26565 |
| 63.31401 | 47.84767 |
| 47.10939 | 41.84815 |
| 37.04615 | 38.50091 |
| 38.05743 | 32.73984 |

**$Fe_2O_3$ – 5 mg/L Humic Acid**

**0.5 mg/L $Fe_2O_3$**

| $C_e$ | $Q_e$ |
|---|---|
| 263.5126 | 53.95569 |
| 100.7065 | 40.54502 |
| 49.99064 | 29.84756 |
| 52.62368 | 24.30105 |
| 16.51883 | 23.01322 |
| 477.6588 | 105.8433 |
| 180.735 | 63.52942 |
| 129.4125 | 55.49397 |
| 112.4847 | 54.5533 |
| 82.80445 | 48.29276 |
| 82.22748 | 45.08927 |
| 925.0392 | 86.75326 |
| 532.5557 | 69.19792 |
| 252.3887 | 60.54433 |
| 208.9641 | 54.57936 |
| 222.547 | 46.63757 |
| 125.638 | 43.41446 |

**1.0 mg/L $Fe_2O_3$**

| $C_e$ | $Q_e$ |
|---|---|
| 108.2932 | 42.76371 |
| 20.92855 | 28.89379 |
| 13.3908 | 24.73517 |
| 29.17572 | 21.46427 |
| 9.346984 | 19.52364 |
| 596.6251 | 92.40134 |
| 272.8978 | 79.58574 |
| 212.3303 | 67.86868 |
| 165.3228 | 59.23532 |
| 184.8408 | 52.79862 |
| 123.8562 | 45.97631 |
| 87.04928 | 38.53314 |
| 887.803 | 108.8377 |
| 510.0466 | 81.38768 |
| 247.867 | 71.09027 |
| 185.9124 | 56.38918 |
| 129.5209 | 49.8234 |
| 76.26213 | 43.84017 |

## APPENDIX 2: SOP for Conducting Adsorption Isotherm Experiments

a. Solutions of TCE should be prepared in autoclaved nanopure water buffered with 0.001 M $KH_2PO_4$ and the pH adjusted to 7 with a 10 M NaOH solution. For acidic isotherms, water should be buffered to pH 3.5 using 0.001 M formic acid. For each isotherm three different concentrations should be prepared (750, 1250, and 2000 µg/L TCE).

b. Place accurately weighed (± 0.1 mg) masses of nanomaterials in the solutions prepared in step (a) for isotherms containing $SiO_2$, $TiO_2$, or $Fe_2O_3$. Mix thoroughly for 30 min.

c. Each set of bottles (different initial concentration) should be accompanied by three blanks (bottles not containing activated carbon) in order to check for any

volatilization, adsorption onto the walls of the bottles, biodegradation of TCE, and to represent the initial aqueous TCE concentration.

d. Place accurately weighed (± 0.1 mg) masses of activated carbon in each of 250 ml glass amber bottles.

e. Add the adsorbate solutions prepared in steps (a) and (b) to each of the isotherm bottles prepared in step c plus three more bottles not containing activated carbon for each initial concentration. Each set of bottles should contain eight bottles with activated carbon and three blanks (i.e., not containing activated carbon). Each bottle should be filled completely to allow no head space, sealed tightly with Teflon lined caps and covered by parafilm.

f. Place the isotherm bottles in a rotary shaker (tumbler) for a period of two weeks in order to attain equilibrium.

g. After equilibration, take 10 mL sample from each bottle to measure its pH. Take another 20 mL sample, filter it through 0.1 μm filter. Dilute the filtered sample and place the solution in a 44 mL vial, filled to the rim. Inject a consistent volume of internal standard (PCE) into each vial. Seal the vials with Teflon lined caps and covered by parafilm. Store the vials in the fridge at 4 C for a period not more than 7 days until analysis or analyze immediately.

h. For adsorption isotherms of TCE in water containing nanomaterials ($SiO_2$, $TiO_2$, or $Fe_2O_3$), repeat steps (a) to (f ) with exception of step (d). In this case, three more bottles containing TCE solution in water not containing nanomaterials should accompany each set to act as blanks.

## APPENDIX 3: SOP for Particle Size Distribution Analysis

a. Switch on Laser Particle Counter (Model PC-2000). A laser beam will appear from the projection box toward the left of the instrument.

b. Place the 250 mL bottle of solution onto the "V" block. Ensure that the bottle is clean prior to placing it onto the "V" block.

c. Set the threshold setting to the 1 μm level, and press the count button. When the counting has stopped, a computer attached to the particle counter shows the particle size distribution of the sample. This provides the number of particles per cubic cm at each size level specified. Specification can be made between 1 μm and 16 μm.

## APPENDIX 4: Quality Control Procedures for Critical Target Parameters

| Parameter | QC Checks | Frequency | Acceptance Criteria | Corrective Action |
|---|---|---|---|---|
| Trichloroethylene Concentration | Initial Demonstration of Precision | Initially | The %RSD must be ≤15% | The source of the problem must be identified and corrected |
| | Initial Demonstration of Accuracy | Initially | The mean recovered concentration(Cx) must be within 15% of the true value | The source of the problem must be identified and corrected |
| | Quality control sample (QCS) from an external/second source | Initially, upon reestablishing calibration/ at least quarterly | QCS should be within 10% of the true value | The source of the problem must be identified and corrected |
| | Initial Calibration | Initially | RF for each concentration level less than 15% of the average RF | Prepare new standards and re-calibrate |
| | Standard calibration check | After every 5 samples (4 samples + method blank) or every 4 samples if method blank is not analyzed at that time | Percent recovery 90-110% | Correct problem; recheck calibration standard; re-check calibration |
| | Method Blank | Two replicates conducted on the first day and two replicates conducted on the last day of the test | < DL | Investigate to find source; re-run blanks |
| | Laboratory sample matrix spike | For every 5% of samples or one within each analysis batch | Recovery must be 80-120% | Investigate to find source and make necessary corrections |
| | Laboratory sample matrix duplicate | For every 5% of samples or one within each analysis batch | RPD must be ±15% | Investigate to find source and make necessary corrections |
| pH | Calibration against 4, 7 & 10 pH standards | Daily | ±0.2 pH units | Recalibrate |
| Temperature | Calibration against standard of known temperature | Daily | ± 2 degrees Celsius | Acquire new thermometer |
| Particle Size Distribution | Testing of Triplicate Samples | Daily | The %RSD must be ≤15% | Investigate to find source and make fresh solutions |